Bulletin of the Seismological Society of America, Vol. 93, No. 2, pp. 674–693, April 2003

Some Observations on Colocated and Closely Spaced Strong Ground-Motion Records of the 1999 Chi-Chi, Taiwan, Earthquake

by Guo-Quan Wang, David M. Boore, Heiner Igel, and Xi-Yuan Zhou

Abstract The digital accelerograph network installed in Taiwan produced a rich set of records from the 20 September 1999 Chi-Chi, Taiwan earthquake (M_w 7.6). Teledyne Geotech model A-800 and A-900A* digital accelerographs were colocated at 22 stations that recorded this event. Comparisons of the amplitudes, frequency content, and baseline offsets show that records from several of the A-800 accelerographs are considerably different than those from the colocated A-900A accelerographs. On this basis, and in view of the more thorough predeployment testing of the newer A-900A instruments, we recommend that the records from the A-800 instruments be used with caution in analyses of the mainshock and aftershocks. At the Hualien seismic station two A-900A and one A-800 instruments were colocated, along with a Global Positioning System instrument. Although the records from the two A-900A instruments are much more similar than those from a colocated A-800 instrument, both three-component records contain unpredictable baseline offsets, which produced completely unrealistic ground displacements derived from the accelerations by double integration, as do many of the strong-motion data from this event; the details of the baseline offsets differ considerably on the two three-component records. There are probably numerous sources of the baseline offsets, including sources external to the instruments, such as tilting or rotation of the ground, and sources internal to the instruments, such as electrical or mechanical hysteresis in the sensors. For the two colocated A-900A records at the Hualien seismic station, however, the differences in the baseline offsets suggest that the principal source is some transient disturbance within the instrument. The baseline offsets generally manifest themselves in the acceleration time series as pulses or steps, either singly or in combination. We find a 0.015-Hz low-cut filter can almost completely eliminate the effects of the baseline offsets, but then information regarding the permanent displacements is lost. The causative mechanisms of the baseline offsets are unknown presently. Hence, it is very difficult to recover the permanent displacements from the modern digital records, although for records close to large earthquakes, the signal-to-noise ratio should theoretically be adequate to obtain ground motions with periods of hundreds of seconds. This study reinforces our conclusion from previous studies that the sources of baseline offsets occurring in digital strong-motion records are very complex and often unpredictable, and that, therefore, it is difficult to remove the baseline effects to maximize the information content of the record. The baseline offsets only affect very long period motions (e.g., $>$20 sec), however, and therefore are of little or no engineering concern.

Introduction

The Chi-Chi, Taiwan earthquake (M_w 7.6, 17:47, 20 September 1999, Universal Time (UT); epicenter at 23.86° N, 120.81° E) produced the largest set of digital strong-motion data ever recorded from a single earthquake (Shin *et al.*, 2000). After this event, scientists from Taiwan and the United States made an intensive effort to make the data available as soon as possible for scientists worldwide. For the mainshock, 441 digital, three-component, free-field, strong-motion records (out of a total of 640 digital acceler-

*Use of trade, product, or firm names is for descriptive purposes only and does not imply endorsement by the U.S. Government.

ographs deployed at the "free-field" sites) were released by the Central Weather Bureau of Taiwan (CWB) (Lee *et al.*, 1999, 2001a). In our previous studies (Boore, 1999, 2001; Wang, 2001; Wang *et al.*, 2001, 2002), we found that displacements derived from near-fault accelerogram recordings of this event show significant drifts when only the mean of the pre-event portion of the record is removed from the whole record. The appearance of the velocity and displacement records suggests that some changes in the relative zero level of the accelerations are responsible for these drifts. These changes, although very small in acceleration, will produce large unrealistic displacements derived from the accelerations by double integration and make it difficult to recover permanent displacements from these digital records. In this study, we refer to the changes in the relative zero level of the accelerations as baseline offsets. High-dynamic-range, broadband, high-resolution digital accelerogram recordings from strong earthquakes have the potential to yield ground displacements accurately over a wide range of frequencies in theory, including those so low that the displacements give the residual, static deformation following an earthquake (called "residual displacement" by Graizer, 1979). The long-period information is of interest to seismologists for unravelling the dynamic process of fault rupture and may be of interest to engineers for designing large structures with very-long-period response.

As far as we know, a robust procedure for the correction of the baseline offsets that can be applicable to digital strong-motion recordings has not been proposed. To develop such a procedure, the specific sources of the baseline offsets must be understood. Among the 441 accelerographs are 22 Teledyne Geotech A-800–A-900A pairs installed at the same site. Comparisons of these colocated records are helpful in understanding the problem of baseline offsets occurring in near-fault records of this event (e.g., Boore, 2001). As one way of contributing to this understanding, we compare carefully the records from three colocated instruments HWA(A-800), HWA019(A-900A), and HWA2(A-900A) installed at the Hualien seismic station. In addition, records from two stations (HWA013[A-900] and HWA014[A-900]) that are relatively very close to the Hualien seismic station are also analyzed. The locations of the sites are shown in Figure 1.

Many researchers have studied the problem of baseline offsets on records from digital instruments (e.g., Amini and Trifunac, 1985; Novikova and Trifunac, 1992; Chiu, 1997, 2001; Boore, 1999, 2001; Wang, 2001; Shakal and Petersen, 2001; Trifunac and Todorovska, 2001). These offsets have been attributed to a number of sources, such as electrical or mechanical hysteresis in the sensor (Iwan *et al.*, 1985; Shakal and Petersen, 2001), misalignment and cross-sensitivity of transducers (Wong and Trifunac, 1977; Todorovska *et al.*, 1995; Todorovska, 1998), distortions produced by the analog-to-digital conversion (Boore, 2003), electronic 1/*f* noise (J. Evans, oral comm., 2002), and ground tilt and rotation (e.g., Bradner and Reichle, 1973; Trifunac and Todorovska, 2001). Boore (2001) argued that similar trends in the displacements from two colocated instruments, TCU129(A-900A) and WNT(A-800) (at a station with a distance-to-fault surface of 2.21 km), triggered by the Chi-Chi mainshock were evidence for permanent ground tilt, and that this caused the baseline offsets at this station. If it is assumed that the baseline offset occurs as a single step, a simple correction can be used based on fitting the linear trend in velocity, after the portion of strong shaking, with a straight line, and then subtracting the slope of the fitted line from the acceleration starting at the time at which the line intersects the zero axis of the velocity trace (Boore 2001; Shin *et al.*, 2001; Wang, 2001; Wang *et al.*, 2001). Applications of this correction scheme to records with strong shaking close to the fault rupture often result in reasonable displacement traces. The baseline offsets can be quite large (on the order of 1 cm/sec^2) and may be associated with ground tilt or ground deformation (F. Wu, oral comm., 2001), in which case they are signals rather than systematic noise. Our study shows that baseline offsets can also occur even for relatively weak motions, and that the simple correction just mentioned cannot remove the baseline offsets. A combination of effects might be related to the level of shaking and to properties of the instrument. The latter is what probably occurred on most of the records that we have studied, and indicates the level of "random" or aleatory uncertainty in the very-long-period displacements. In this article we present a detailed study of records from colocated and closely located instruments to explore further the sources causing the baseline offsets.

Data Sources and Processing

Except as discussed later, the data we used came from Lee *et al.* (2001a). The A-800 accelerograph is a 12-bit digital data recorder and contains three Geotech model S-110 accelerometers mounted orthogonally inside a cast aluminum base. The accelerographs are equipped with piezoelectric transducers with a low-cut frequency of 0.02 Hz; in addition, the datalogger includes a 0.1-Hz low-cut filter (J. Kerr, oral comm., 2001; W. H. K. Lee, written comm., 2001). Data are stored in Complementary Metal Oxide Semiconductor (CMOS) static random access memory (RAM) using a nondistorting format without data compression. The A-900 instruments are upgraded with 16-bit resolution, new Geotech DC Force Balanced Accelerometers (FBA), and the capability to use a Global Positioning System (GPS) receiver for time synchronization. The important differences between the A-900/A and A-800 models are that the A-900 model uses a Geotech model S-220 FBA, which has a flat response to DC and does not include a low-cut filter. The A-900A accelerograph is an improved version of the A-900, which has the following two additional features: it is submersible to 2 m, and it has a real-time digital data stream in U.S. Geological Survey (USGS) Real-Time Digital Telemetry System format. On the A-900 and A-900A instruments, a GPS-1 receiver can be used to synchronize the internal timing (http://www.geoinstr.com/A-900.htm). The dynamic

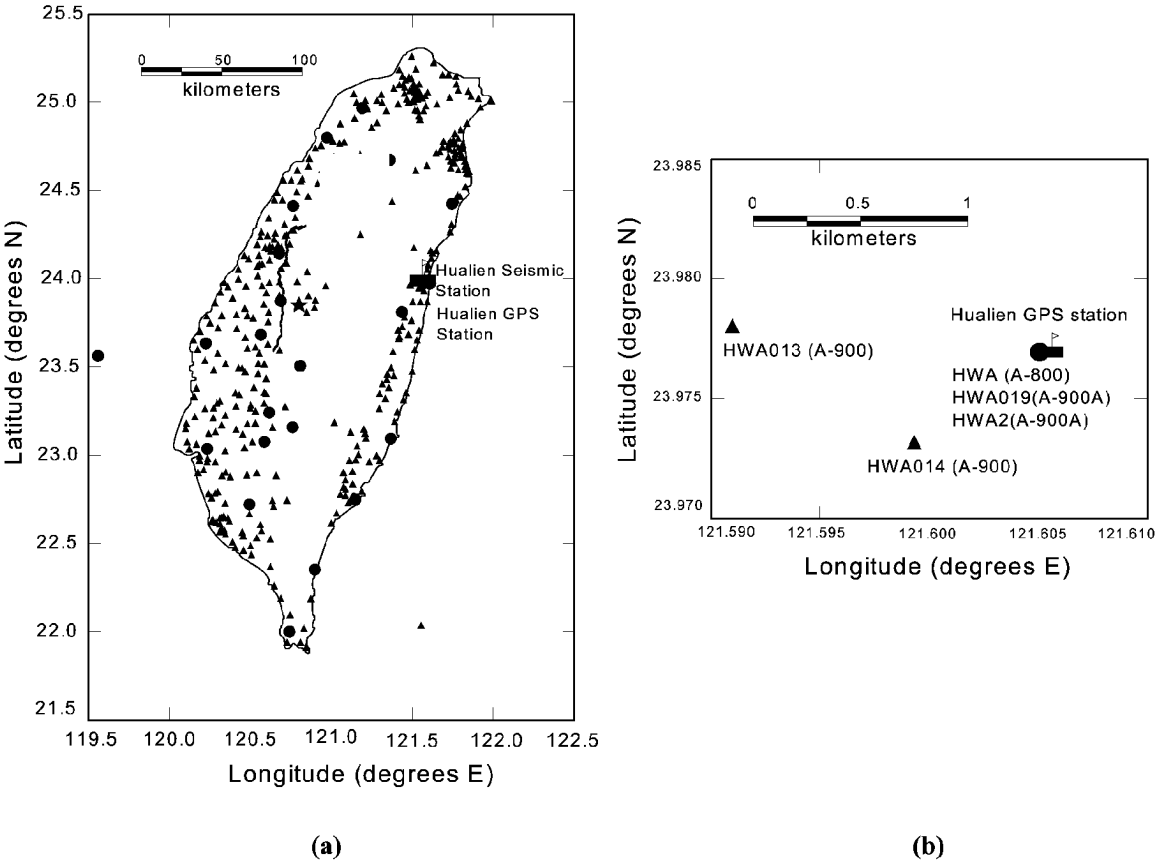

Figure 1. Map showing the locations of accelerographs mentioned in this article. (a) The star indicates the epicenter of the Chi-Chi mainshock, and the line represents the causative Chelungpu fault. The solid triangles represent the 441 accelerographs (two are on the small islands off the main island) for which records were released by the CWB (Lee *et al.*, 1999, 2001a). The solid circles represent the 22 colocated A-800–A-900A pairs, for which locations and recorded peak ground accelerations (PGAs) are listed in the Appendix. The flag marks the Hualien GPS station. (b) The enlargement around the Hualien seismic station. Two A-900A (HWA019 and HWA2) and one A-800 (HWA) accelerographs were installed at the Hualien seismic station, along with one GPS instrument. The coseismic displacements obtained from the GPS measurements are -0.8 ± 0.9 cm, 3.7 ± 0.3 cm, and -21.3 ± 0.3 cm for the north–south, and east–west components, respectively (Yu *et al.*, 2001). The horizontal distance between the Hualien station and the HWA013 station is 1.45 km, between the Hualien station and the HWA014 (A-900) station is 0.72 km, and between the HWA013(A-900) station and HWA014 station is 1.0 km.

ranges ($= 20 \log [A_{max}/A_{min}]$, where A_{max} and A_{min} are the largest and smallest amplitudes that can be recorded) of the A-800 and A-900/A accelerographs equal 72 dB and 92 dB, respectively. The data resolutions are 0.489 and 0.0598 Gal/count for the 12-bit A-800 and the 16-bit A-900/A accelerographs (Liu *et al.*, 1999). Some physical parameters of the A-800 and A-900/A models are listed in Table 1.

All of the A-800 and A-900/A accelerographs have three channels, and the trigger algorithm allows a threshold setting for individual channels. In practice, however, a common triggering mechanism is used for the three channels, and all three channels are recorded at the same time (W. H. K. Lee, written comm., 2001). Both the A-800 and A-900/A models use a trigger algorithm and a buffer, so that the pretrigger part of the ground motion is captured, which is very important for accurately obtaining the zero reference level of accelerogram. Only a fraction of the CWB free-field accelerographs are equipped with a GPS timing device, and the timing for most of the strong-motion records is based on the accelerograph's internal clock, which may not be synchronized to UT. The five instruments studied in this article were not equipped with GPS units. To make detailed comparisons of the ground accelerations, velocities, and displacements, it is necessary to provide a common time base for all of the records. Time corrections were determined for most of the records of this event by Lee *et al.* (2001a), and the results were used in this research. Basic information regarding records used in this article, including the accelero-

graph locations, distance to epicenter and rupture, absolute UT of the record start and *P*-arriving, record length, and instrument models, are listed in Table 2.

A preliminary baseline correction has been applied to all acceleration records used in this study by removing the mean determined from a segment of the pre-event portion of the original record from the whole original record—this guarantees that the velocity will be practically zero near the beginning of the record. For simplicity of expression, the resulting accelerations are called "uncorrected" accelerations, although an initial correction has been applied. In turn, velocities and displacements obtained by single and double integration of the uncorrected accelerations are called uncorrected velocities and uncorrected displacements, respectively.

Study of Records from Colocated Instruments

An indication that there are systematic differences between the A-800 and A-900A records comes from the differences of peak ground accelerations (PGAs) from the 22 colocated A-800 and A-900A instruments. The specific information for the 22 pairs is listed in the Appendix. Figure 2 illustrates the differences of PGAs recorded by the 22 colocated A-900A and A-800 records. The peak accelerations for the A-800 instruments tend to be smaller than those from the A-900A instruments. Note that the filter used within A-800 models is a 0.1-Hz low-cut filter, which has nearly no effect on PGA theoretically. We have made a more detailed study of the records from the three colocated instruments at the Hualien seismic station. This station is classified as a soil site, National Earthquake Hazards Reduction Program (NEHRP) class D (Building Seismic Safety Council, 1998; Lee *et al.*, 2001d), with a distance to the epicenter of 83 km. The instruments HWA(A-800) and HWA019(A-900A) were bolted down to a single concrete seismic pier strictly according to the manufacturer's specifications. The surface size of the seismic pier is 2.0 m by 3.0 m, with a height of 0.6 m. The HWA2(A-900A) instrument was a unit that was deployed in the Hualien station temporarily and happened to record the Chi-Chi event. It was not bolted down at the time of the Chi-Chi event. The HWA(A-800) and HWA019(A-900A) models were separated by about 1.0 m, and the HWA2(A-900A) model was placed on the same

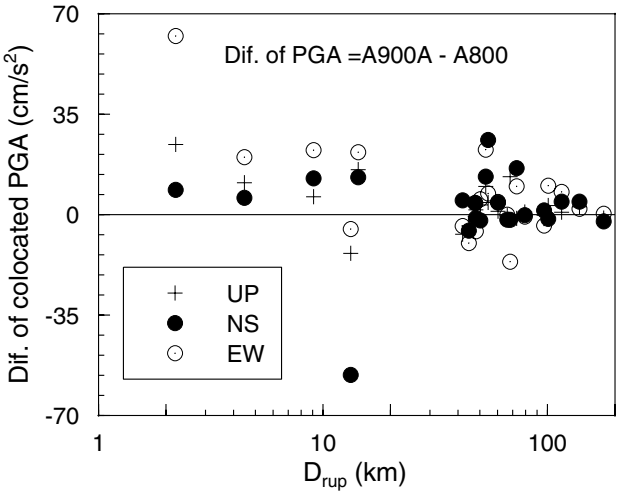

Figure 2. Differences (Dif.) of peak ground accelerations (PGAs) recorded by the 22 colocated A-900A–A-800 accelerographs. The ordinate represents the difference of PGAs recorded by colocated A-900A and A-800 instruments; the abscissa represents the shortest distance from the station to the fault rupture surface. The different marks in the figure represent the different components of ground motions.

Table 1
Characteristics of A-800 and A-900/A Type Accelerographs (Liu *et al.*, 1999)

Model	Resolution	Full Scale	Digital Counts (cnt)	Dynamic Range	Sampling Rate (sps)	Memory
A-800	12-bit	1 g	2,048 cnt/g	72 dB	200	1 MB
A-900/A	16-bit	2 g	32,768 cnt/g	92 dB	200	8 MB

Table 2
Basic Information of Records Studied in This Article (Lee *et al.*, 2001a)

Station	Site Condition (NEHRP)	Lat. (°N)	Long. (°E)	Elevation (m)	Epdist. (km)*	Drup† (km)	Corrected Record Start Time (UT, h:m:s)	Corrected P-Arrival Time (UT, h:m:s)	Pre-event Portion (sec)	Length of Record (sec)	Instrument Model
HWA	D	23.977	121.605	16	83	54.47	17:47:28.956	17:47:31.381	2.425	103	A-800
HWA2	D	23.977	121.605	16	83	54.47	17:47:16.481	17:47:31.381	14,900	133	A-900A
HWA019	D	23.977	121.605	16	83	54.47	17:47:16.143	17:47:31.381	15.239	133	A-900A
HWA013	D	23.978	121.591	9	81.6	53.08	17:47:15.104	17:47:31.159	16.655	134	A-900
HWA014	D	23.973	121.599	3	82.4	54.02	17:47:17.744	17:47:31.279	13.535	131	A-900

*Epdist, distance (km) from Chi-Chi epicenter (23.8603° N, 120.7995° E).
†Drup, the shortest distance between the station and the fault rupture surface.

seismic pier (W. H. K. Lee, written comm., 2001, 2002). A GPS instrument was also installed at the Hualien seismic station. The coseismic displacements estimated from the GPS measurements are -0.8 ± 0.9 cm, 3.7 ± 0.3 cm, and -21 ± 0.3 cm for the up–down (negative represents the down direction), north–south (positive represents the north direction), and east–west (negative represents the west direction) components, respectively (Yu *et al.*, 2001).

Figure 3 illustrates the uncorrected accelerations of the three colocated instruments HWA(A-800), HWA019(A-900A), and HWA2(A-900A). Unless indicated otherwise, all of the time series illustrated in this study are aligned according to the corrected absolute start times (UT) of the records, as given in Table 2. The acceleration time series of the two A-900A instruments (HWA019, HWA2) coincide well in both the amplitude and phase during the whole time series according to our careful observations of the superimposed accelerograms. Some striking differences, however, are apparent by visual comparison without overlay between the A-800 and A-900A accelerograms for all three components, particularly for long-period components. Note again that the accelerations of the A-800 have been filtered with a 0.1-Hz low-cut filter within the instrument. Figure 4 illustrates the differences of the accelerograms of the east–west components of HWA019 and HWA2. Before calculating the differences, the first 62 points (or $62/200 = 0.32$ sec) of HWA019-EW have been cut off so that the two traces are aligned according to the time corresponding to the PGA. The difference trace oscillates around the relative zero level and perfectly mimics the accelerograms in the individual time series. This implies that there are some small differences in the gains of the two A-900A instruments.

Integrating to velocity and displacement provides a way of comparing the longer period components of motion. The results are shown in Figure 5. At a sufficiently long time after the strong shaking, the ground velocities should oscillate at about the zero level and be essentially zero (the shaking has ceased), and the displacement-time series should be constant and equal to the permanent displacement produced during the earthquake. However, what we see as a digital "record" is not the actual time series of the ground accelerations, but the response or output of the accelerograph to the input motions, in combination with systematic errors. As illustrated in Figure 5, our expectations of what the ground motion should be are not met for the colocated records at Hualien station; the latter portions of velocities do not oscillate around the zero level, and the displacements for all records show no signs of leveling off at the end of the records (at a time well beyond the expected duration of strong shaking), particularly for the traces of the A-800 instrument. These problems are due to what we call baseline offsets—small changes in the reference level of the accelerograms. Baseline offsets occur in both the A-800 and A-900A records, but they seem more severe for the A-800 records. Because the HWA2(A-900A) instrument was not bolted down, we can not eliminate the possibility that some small slipping

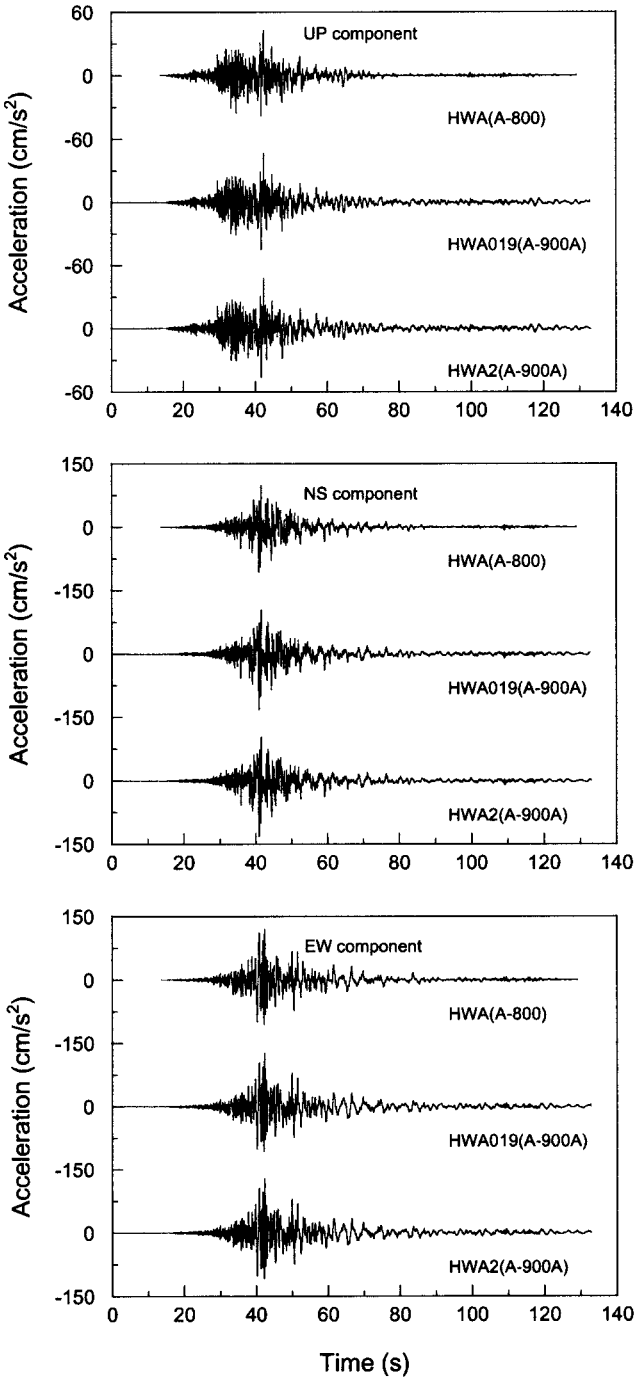

Figure 3. Comparison of the three-component acceleration time series obtained from the three colocated instruments HWA(A-800), HWA019(A-900A), and HWA2(A-900A). The mean determined from a segment of the pre-event portion of the original record was removed from the whole record. These records are aligned according to the corrected record start times (absolute UT, listed in Table 2).

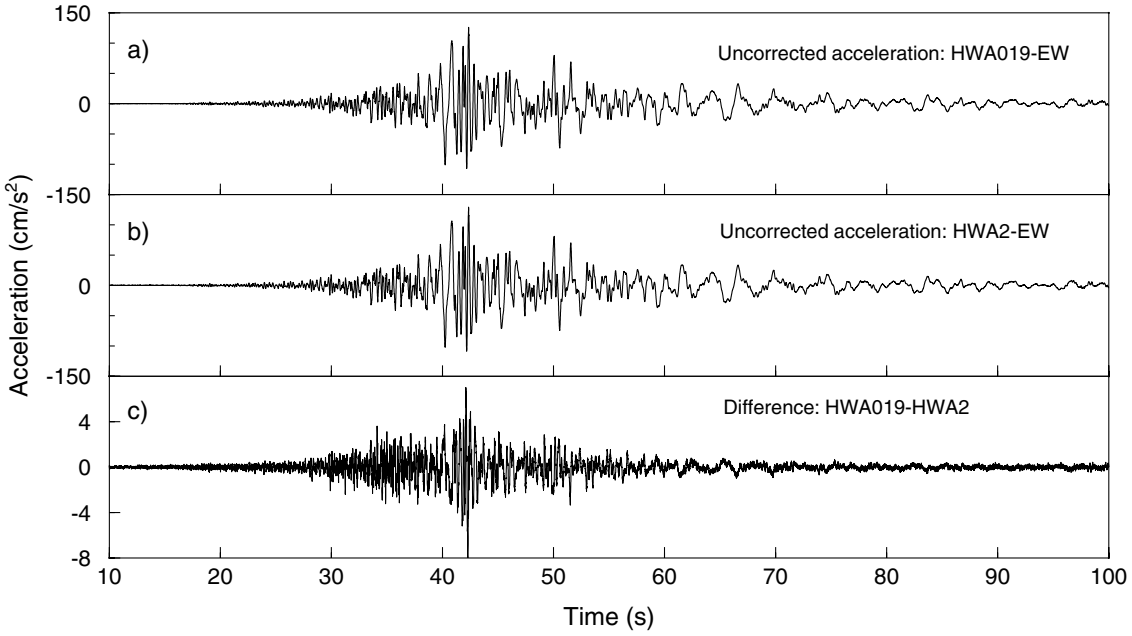

Figure 4. Acceleration time series and differences of the time series for the east–west components of records from colocated instruments HWA019 (A-900A) and HWA2(A-900A). (a) Acceleration time series of HWA019-EW. (b) Acceleration time series of HWA2-EW. (c) Differences of the two accelerograms: HWA019–HWA2. The accelerograms have been aligned such that the peak acceleration occurs at the same time; this was accomplished by deleting the first 62 points (0.32 sec) of HWA019-EW.

or rotation occurred for this instrument during the shock, which could lead to an offset of the baseline. Because the station is far from the epicenter (the epicentral distance is 83 km) and the ground motions at this site were not very strong (up, 47.7 cm/sec^2; north–south, 132.2 cm/sec^2; east–west, 129.0 cm/sec^2), however, we think that the possible slipping or rotation of the instrument would have been very small, if it occurred at all. At present, further research on the possible slipping or rotation is nearly impossible. Hence, we will not discuss the possible slipping or rotation of HWA2 in the following analysis.

The previous observations are consistent with accumulating experience that the outputs of high-quality digital instruments are often plagued by baseline problems (e.g., Boore, 2001; Boore *et al.*, 2002; Wang, 2001; Wang *et al.*, 2001). The differences in the trends of the displacements for the same component of motion on the three colocated instruments indicate that the baseline offsets are not the same for all instruments, as would be the case if the offsets are caused by ground rotation or ground tilt, either transient or permanent (Trifunac and Todorovska, 2001), which suggests that the source of the baseline offsets must be internal to each instrument. The trends in the displacement records from the A-800 instrument imply a significant amount of long-period energy in the record. This apparent energy was probably introduced into the record during or after the analog-to-digital (A/D) conversion and not from actual motion of the ground, indicating that the problem is in the datalogger. We are fairly certain of this because the A-800 instrument uses a low-cut piezoelectric transducer and also includes a 0.1-Hz low-cut filter before the A/D conversion (J. Kerr, oral comm., 2001; W. H. K. Lee, written comm., 2001); we assume that electronic noise in the filters is small enough not to produce the long-period trends.

The latter portions of the velocity traces of the up and north–south components of the HWA(A-800) instrument have the form of a constant step with an amplitude of about 3 cm/sec occurring at about 45 and 65 sec, respectively (Fig. 5a,c). Such a step could be produced by a short-lived, pulse-like offset in the baseline of the acceleration trace; this would give an unrealistic displacement that grows linearly with time at the end of record (Fig. 5b,d). The east–west component velocity trace of the A-800 instrument tends to diverge from velocity traces of the A-900 instruments even starting from the initial arrival time (Fig. 5e). The velocity traces from the two A-900A recordings show almost no differences for the UP and NS components (Fig. 5a,c), and only slight differences in the amplitudes for the EW component at times after the strong shaking has ceased (Fig. 5e). Although the differences in the velocity traces of the two A-900A models are slight, however, the very small differences are enlarged in the displacement traces. The displacement traces from the both A-900A instruments tend to diverge even starting from the initial arrival time, and significant divergences occur after about 50 sec (Fig. 5b,d,f).

Estimates of the coseismic displacement calculated

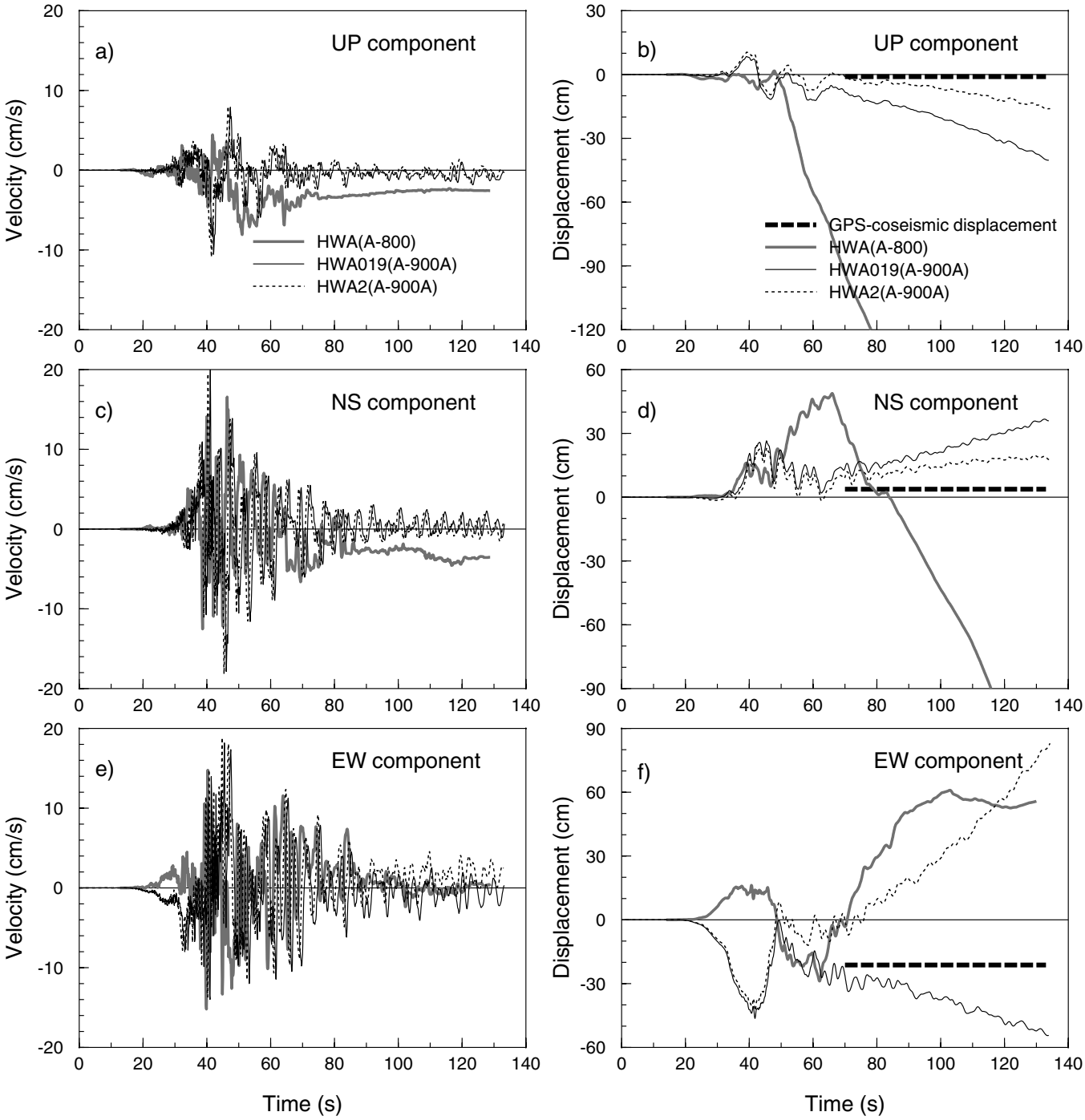

Figure 5. Comparison of uncorrected velocities and displacements of the three co-located instruments HWA(A-800), HWA019(A-900A), and HWA2(A-900A). The uncorrected velocities and displacements were obtained by single and double integration of uncorrected accelerations. The GPS estimates of the coseismic displacements (heavy dashed lines) are obtained from a GPS instrument colocated with the accelerographs (Yu *et al.*, 2001).

from the colocated GPS measurements are also illustrated in Figure 5. We say "estimates" because the values were obtained as the difference in GPS measurements made one day before and one day after the Chi-Chi mainshock (the Hualien GPS station is a continuously recording GPS station) (S.-B. Yu, written comm., 2001). The values must contain pre- and postseismic motions, as well as coseismic motion. The postseismic motion could be influenced by fault creep after the mainshock and permanent displacements produced by a lot of aftershocks. Shortly after the mainshock (17:47, 20 September 1999), a series of large- and moderate-magnitude aftershocks occurred, e.g., aftershocks at 17:57 (m_L 6.4), 18:03 (m_L 6.6), 18:21 (m_L 5.2), 18:32 (m_L 5.1), 18:34 (m_L 4.9), 19:40 (m_L 5.3), 19:57 (m_L 5.2), 20:21 (m_L 5.2), 21:27 (m_L 5.0), 21:46 (m_L 6.6) of 20 September 1999 (Lee *et al.*, 2001b,c). In just the first 6 hr after the mainshock, thousands of aftershocks occurred and generated about 10,000 records (Lee *et al.*, 2001c). According to the work of Yu *et al.* (2001), the preseismic and postseismic displacements of these events are insignificant compared with the displacements produced during the mainshock, particularly for sites far from the causative fault. Considering that the Hualien station is far from the epicenter of this event (the epicentral distance is 83 km), we assume that the GPS measurements are a good estimate of the actual coseismic motion, and from now on we will refer to the GPS values as "coseismic" displacements without qualification. It can be seen from Figure 5 that all of the final displacements integrated from acceleration time series are much larger than the corresponding coseismic displacements, particularly for the A-800 records.

For further analysis of the difference in the amplitude and frequency content of the three colocated records, we studied their Fourier spectra and response spectra. Figures 6 and 7 show the Fourier acceleration spectra and the 5%-damped pseudoacceleration response spectra obtained from the uncorrected accelerations of the three colocated instruments, respectively. The Fourier spectra from the two A-900A models agree well with one another for frequencies greater than 0.01 Hz for the east–west component and 0.02 Hz for the up–down and north–south components. There are significant differences between Fourier acceleration spectra of the A-800 and A-900A models for frequencies less than 0.1 Hz, however. This is partially because of the 0.1-Hz low-cut filtering within the A-800 model. To capture the differences caused by the drifts in the displacements, the response spectra have been computed for oscillator periods up to 1000 sec (before computing the response spectra, enough zeros were added to the end of the acceleration time series so that the total duration exceeded the oscillator period). The response spectra from the two A-900A records agree very well for periods less than 100 sec. The differences between the response spectra of A-900A and A-800 instruments begin to appear at periods as short as 5 sec (Fig. 7a,b), however. That means the bandwidth of the A-800 model is very limited.

These comparisons of the three colocated records in accelerations (Figs. 2 and 3), velocities and displacements (Fig. 5), Fourier spectra (Fig. 6), and response spectra (Fig. 7) suggest that there are some problems with the response and calibration of the A-800 type accelerographs. The analysis discussed in the preceding paragraph seems to confirm the advice of the publishers of the Chi-Chi data—"users are advised not to use the A-800 accelerograph records" (Lee *et al.*, 2001a). This caution was not based on detailed comparisons such as we have shown here, but rather on the fact that

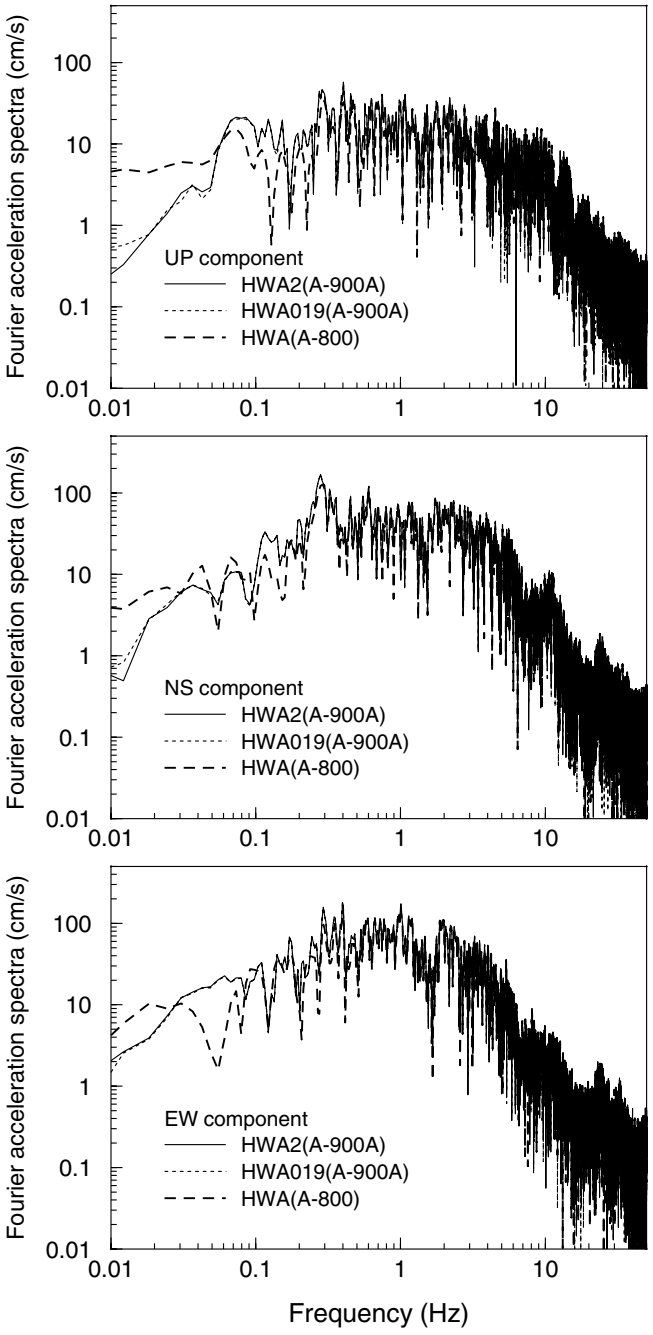

Figure 6. Fourier acceleration frequency spectra calculated from the uncorrected accelerations recorded by the three colocated instruments HWA(A-800), HWA019(A-900A), and HWA2(A-900A).

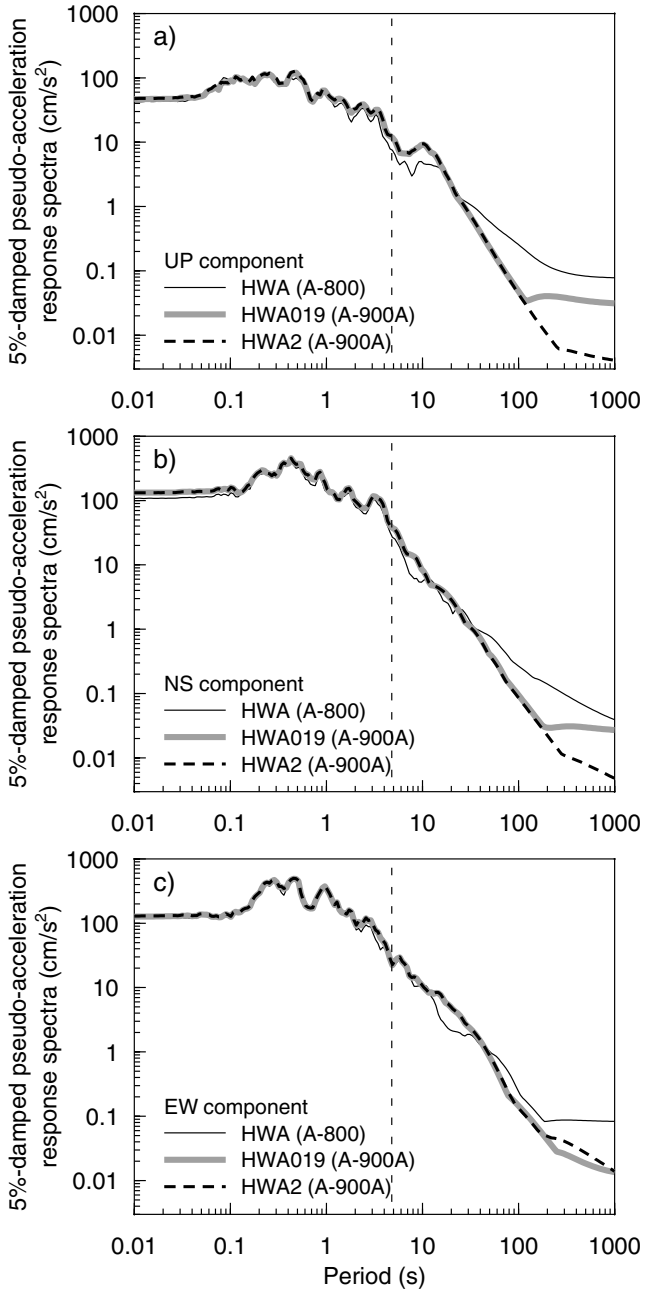

Figure 7. Five percent-damped pseudoacceleration response spectra calculated from uncorrected accelerations recorded by the three colocated instruments HWA(A-800), HWA019(A-900A), and HWA2(A-900A). Before computing the response spectra, zeros were added to the end of the acceleration time series so that the total duration exceeded the oscillator period.

the A-800 instrument was an older model, and had not been rigorously tested by the team that installed the strong-motion network of Taiwan. Furthermore, most A800 accelerographs are at station sites equipped with more modern digital accelerographs. In view of our detailed comparisons, we suggest that records from A-800 instruments be used with caution, or not at all, in analyses of the long-period information of either the mainshock or the aftershocks. Of the 441 stations that recorded the mainshock, about 10 had records only from A-800 instruments; for this reason, ignoring the A-800 records will have little impact on studies of the mainshock.

Study of Records from Closely Spaced A-900/A Instruments

This section compares the records of three closely spaced instruments: HWA013(A-900), HWA014(A-900), and HWA019(A-900A) (and its colocated instrument HWA2[A-900A]). The specific locations of the three sites are shown in Figure 1b and listed in Table 2. It is noted that the instruments HWA013 and HWA014 were bolted down according to the manufacturer's specification. In fact, except at the telemetered stations, all CWB free-field accelerographs are housed in a special hut with a concrete pad in the ground, and the accelerograph was bolted down to the concrete pad by technicians trained by the accelerograph's manufacturer (W. H. K. Lee, written comm., 2002). A typical station of the Taiwan Strong-Motion Instrumentation Program (TSMIP) consists of a concrete pad and a fiberglass hut to provide shelter for the accelerograph. The coupling between the concrete pad and the ground is enhanced by eight 100-cm stainless steel rods. One end of these rods is cemented into the pad, and the other end penetrates the ground (Liu *et al.*, 1999). The thin instrument pad is designed to minimize the soil–structure interaction effects of the pad on recording. Peak ground accelerations, the times for the first and last exceedences of 50 cm/sec^2, and a bracketed duration with a threshold of 50 cm/sec^2 are listed in Table 3. The three stations are located on soil-site conditions (classified as NEHRP class D) (Lee *et al.*, 2001d). The greatest horizontal distance between any two sites is less than 1.5 km (Fig. 1b). The elevations of the three sites are 16 m (Hualien station), 9 m (HWA013), and 3 m (HWA014), respectively. The epicentral distances are about 83 km, and the shortest distances to the fault are about 54 km as listed in Table 2. Thus site-to-site differences in the ground motion due to source and path effects should be minor. We expect the differences among the records at the three sites to be small, at least for longer periods, as noted subsequently.

If a set of stations is spaced at distances small compared with the wavelengths within a frequency band of interest, and if the variation of material properties is not appreciable within the immediate vicinity of the array, there should be little distortion of a long-period disturbance as it crosses the array. For example, for periods greater than about 3 sec, with wavelengths of approximately 10 km or longer, there should be little distortion of signal amplitudes across an array of the dimension of 1 to 2 km or less. Any differences in long-period amplitudes must then be attributed to instrumental or processing errors (Hanks, 1975; Abrahamson and Sykora, 1993; Field and Hough, 1997; Evans, 2001). Because of the intrinsic smoothing process of integration and the relative

Table 3
Peak Ground Acceleration (PGA), T_1, T_p and T_2, and Duration of Studied Records

	PGA (cm/sec^2)			T_1 (sec)*			T_p (sec)*			T_2 (sec)*			Duration (sec)†		
	UP	NS	EW	UP	NS	EW	UP	NS	EW	UP	NS	EW	UP	NS	EW
HWA	42.590	−107.672	119.135		22.36	25.31	29.38	27.93	29.34		32.35	38.12	0.0	9.99	12.81
HWA2	47.729	−132.190	129.080		35.22	37.22	42.04	40.59	42.05		46.40	51.84	0.0	11.18	14.63
HWA019	46.792	−133.568	126.456		35.83	39.78	42.35	40.90	42.36		47.02	51.62	0.0	11.19	11.84
HWA013	61.197	−114.156	139.727	42.67	40.15	40.59	42.69	41.64	42.48	42.70	45.96	52.58	0.03	5.81	11.99
HWA014	−39.296	−90.113	101.545		37.87	38.35	38.75	42.66	39.91		45.99	48.39	0.0	8.12	10.04

*T_1, T_p, and T_2 represent the time that absolute value of acceleration first exceeded 50 cm/sec^2, got the peak value (PGA), and finally exceeded 50 cm/sec^2, respectively. The times are counted from the beginning of the record.

†Duration = T_2–T_1, a bracketed duration with a threshold of 50 cm/sec^2.

increase in the long-period content of the time series, the ground displacements should be more coherent than the ground velocities, which in turn should be more coherent than the ground accelerations. Because of this and the small interstation spacing, we assume that the actual ground displacements at all of the three closely spaced stations were nearly identical.

Figure 8 shows the uncorrected displacements of the four A-900/A instruments. Calculations of the relative time delays for *P*-wave arrivals between the three stations found that the delays were smaller than 0.3 sec; therefore, no correction for these differences was made to align the traces with one another. The graphs in the left column were produced using the "official" distribution of Lee *et al.* (2001a). In preparing the official data Lee *et al.* removed from the whole time series the DC offset computed from 1 sec after the start of the record to 1 sec before the *P*-wave arrival. They stored the DC-corrected data as integers, using a truncation subroutine to convert from floating point to integers (W. Lee, written comm., 2002). This procedure leads to a small error in the data. For example, if the mean had been 57.4 counts, a value of 58 counts would have been stored as int(58–57.4) = 0 rather than 58–57.4 = 0.6. After we realized this, we obtained from W. Lee (written comm., 2002) the data before the DC correction had been applied to see if the results of processing the two sets differed from one another. The uncorrected displacements of using these data are shown in the right column of Figure 8. Comparing the left and right columns of Figure 8 shows that the displacements can be markedly different. The overall conclusions to be discussed next, however, are not affected by which set of data is used. We call the data from Lee *et al.* (2001a) the "2001CD" data, and those from W. Lee (written comm., 2002) without the DC offset correction, we call the "2001CDxmean" data ("xmean" = "without mean"). Both the 2001CD and the 2001CDxmean data are given in digital counts, which we converted to acceleration units (cm/sec^2) during our processing.

The displacement traces are slightly different from one another during the first 50 sec for all three components, particularly for the displacements of the two colocated instruments. Beyond about 50 sec, however, the displacement traces begin to diverge significantly. The trends in some displacement traces appear to be parabolic, suggesting a step change in the acceleration baseline, and some are nearly linear, as would be caused by a short-duration pulse in the acceleration baseline. Moreover, the characteristics of the trends (e.g., linear or nonlinear) are different for the same components of the different instruments, as well as for the different components of the same instrument. The form of the trend in displacement gives some information about the cause of the baseline offsets, but it does not provide enough information to correct unambiguously for the baseline offsets. We conclude that the baseline offsets strongly depend not only on the instrument, but also on the particular component for each instrument. We also note that the differences of the trends in the displacements of the EW components are even larger for the colocated instruments (HWA019 and HWA2) than for the closely spaced, but not colocated instruments (HWA019 and HWA013, HWA019 and HWA014).

When we first prepared Figure 8, using only the 2001CD data, we noticed that the EW displacements for the stations HWA019 and HWA013 are in close agreement for the whole time series (Fig. 8e), even though the stations are not colocated. We thought that this suggested a common origin for the baseline offsets and intepreted the lack of correlation for other components to indicate that any noninstrumental offsets are often masked by instrument- and component-specific baseline offsets. Unfortunately, the results from the 2001CDxmean data no longer show agreement between the EW components at HWA013 and HWA019 (Fig. 8f). Although we still believe that effects of true ground motion can be masked by other effects, we cannot use the comparisons in Figure 8e as evidence for the common origin of some of the trends seen in displacements.

In an attempt to understand the differences in displacements for the 2001CD and 2001CDxmean data sets, we studied the result of subtracting the acceleration time series for the two data sets. An example is shown in Figure 9, for HWA019 EW. The top graph shows the difference of the acceleration times series straight from the datasets, before removing the pre-event mean and converting to units of acceleration. The difference in the acceleration time series resembles noise randomly distributed between values of ±0.5

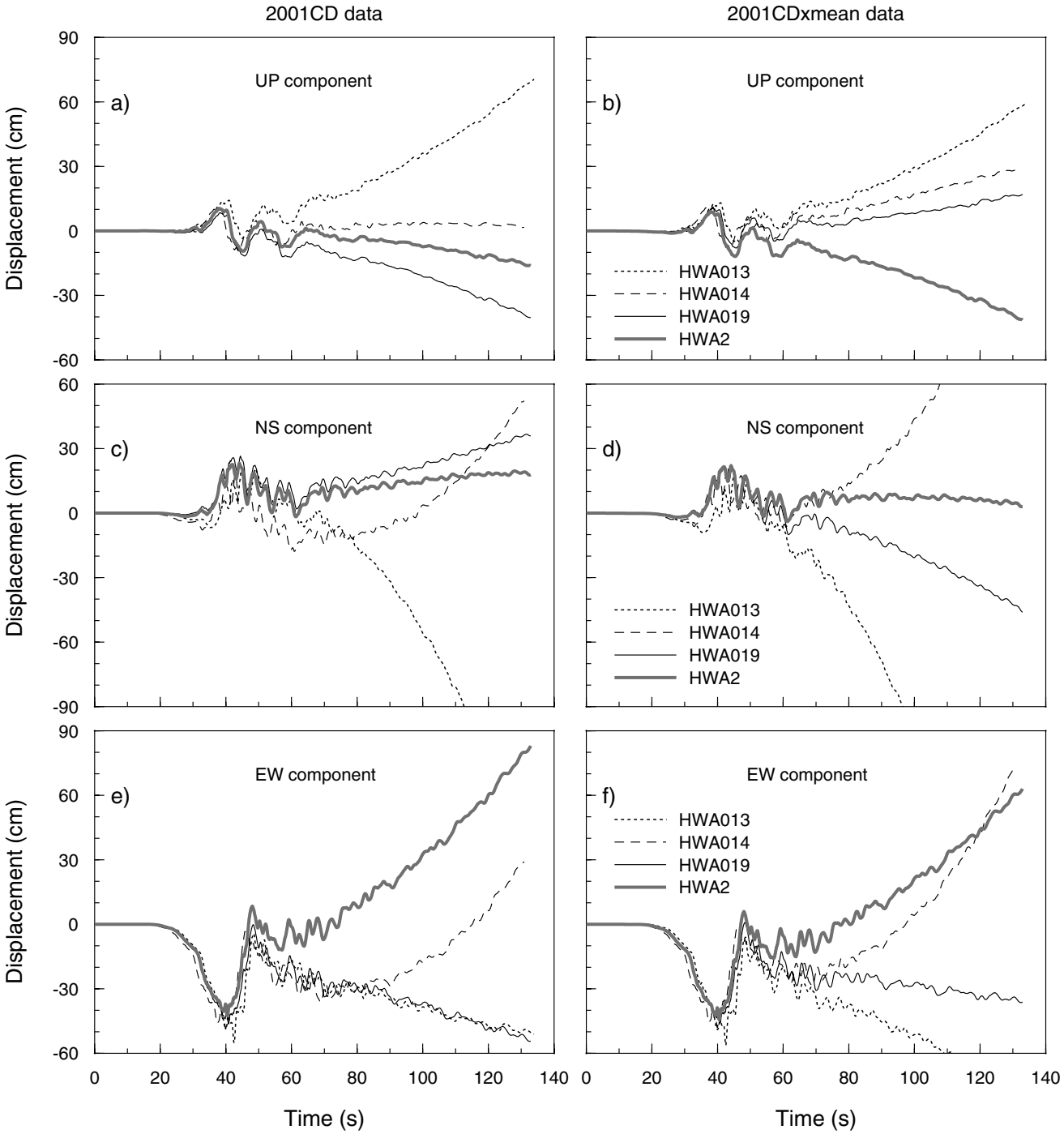

Figure 8. Comparison of uncorrected displacements obtained from four closely spaced instruments HWA013(A-900), HWA014(A-900), HWA019(A-900A), and HWA2(A-900A) (HWA2 and HWA019 are colocated). The displacements are obtained from doubly integrated uncorrected accelerations. Note that traces are not adjusted for travel-time differences. The results in the left and right columns were obtained from 2001CD data (Lee *et al.*, 2001a) and 2001CDxmean data supplied by W. Lee (written comm., 2002), respectively. (See text for more discussion.)

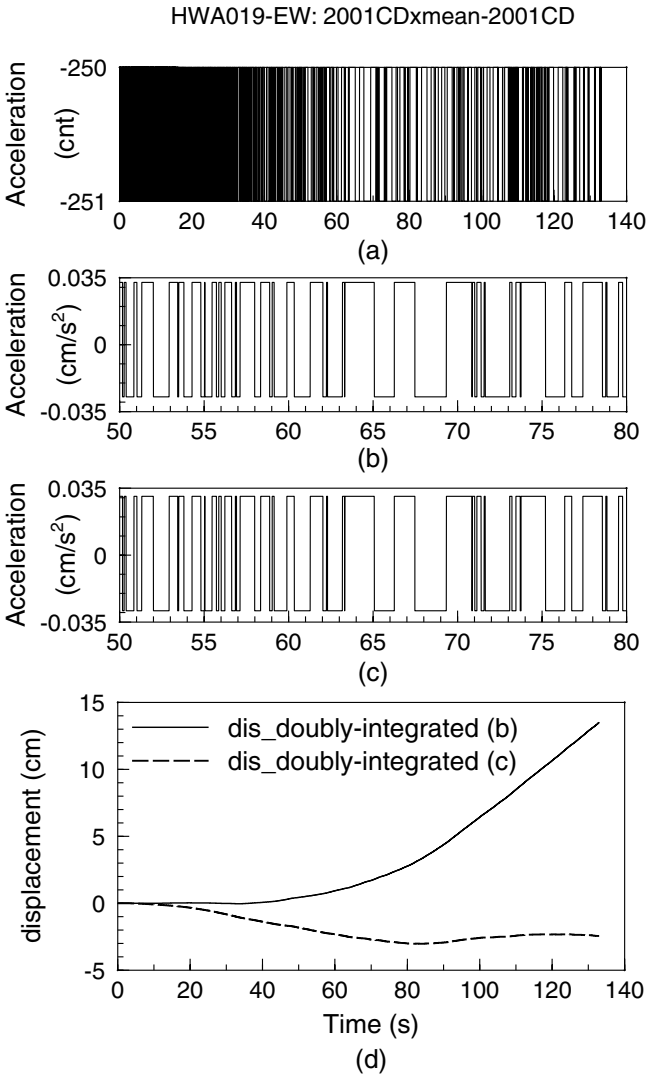

Figure 9. An example of differences between 2001CDxmean data and 2001CD data. (a) Acceleration differences of HWA019-EW between HWA2001CDxmean data and 2001CD data in digital counts (cnt), before our removal of pre-event means. (b) Differences of accelerations corresponding to the displacements (HWA019-EW) illustrated in Figure 8e and f in cm/sec^2; the mean of the pre-event portion of the time series has been removed from the whole time series and to facilitate comparison with the next time series, only a part of whole time series is illustrated. (c) The time series in graph b after removing the overall mean (0.0018 cm/sec^2). (d) Solid line, displacements obtained from double integration of the random noise shown in graph b ($d_{\text{end}} = 13.5$ cm); dashed line, displacements obtained from double integration of the random noise after removing the overall mean of 0.0018 cm/sec^2 (graph c) ($d_{\text{end}} = -2.4$ cm).

counts. Without the truncation operation used in producing the 2001CD data, the difference in the acceleration time series should be a constant equal to the DC correction. A portion of the difference time series is plotted in Figure 9b at an expanded timescale, after removing the mean of the pre-event means from each time series. The overall mean of the difference is not quite 0.0. Removing the mean (0.0018 cm/sec^2) results in the difference time series shown in Figure 9c. The displacement discrepancies shown in Figure 8 between the 2001CD and the 2001CDxmean datasets apparently comprise two parts: the double integration of zero-mean noise distributed between ± 0.5 counts (a double-random walk), and the double integration of the small DC offset. The contributions of both of these is shown as the solid line in Figure 9d; the displacement is equal to that computed from the left and right columns in Figure 8. The contribution of the zero-mean noise to the displacement (shown by the dashed line in Fig. 9d) is much smaller than the contribution of the small DC offset.

Similar analysis for the other time series shows in all cases that the displacement due to the double-random walk is smaller (usually much smaller) than the displacements due to the nonzero DC offset. The small values for the final displacements due to the double-random walk process are consistent with theory. Boore *et al.* (2002) give the following formula (A4 in their article) for the standard deviation of the final displacement (d_{end}) produced by double integration of random noise:

$$\sigma_{d_{\text{end}}} = \sqrt{\frac{T^3 \Delta t}{3}}\, \sigma_a \tag{1}$$

where T and Δt are the duration of record integrated and the time spacing between samples, respectively, and σ_a is the standard deviation of the noise process. For white noise randomly distributed between the two integer values $-Q/2$ and $+Q/2$, where Q is the quanta of acceleration corresponding to one digital count (0.06 cm/sec^2 in our case), this is

$$\sigma_a = Q/2 \tag{2}$$

Inserting appropriate numbers ($T = 134$, $\Delta t = 0.005$, $Q = 0.06$ cm/sec^2) into equation (1) gives $\sigma_{d_{\text{end}}} = 1.9$ cm, which is much smaller than the differences in final displacements from the left and right columns of Figure 8 (our numerical simulations, not shown here, confirm the result of using equations 1 and 2).

The source of the nonzero DC bias is not certain, but is probably associated with the truncation process involved in the removal of the DC offset in the 2001CD data, as discussed earlier. Recall that the mean determined from the pre-event portions of both the 2001CDxmean and 2001CD datasets has been removed, so some of the effect of truncation contained in the 2001CD data has been taken into account. The remaining amount of DC is for the mean of the overall time series and is not necessarily the same as that from the pre-event portion of the time series. We can conclude that the random errors introduced into the 2001CD data (Lee *et al.*, 2001a) by the process of DC offset correction will not produce large displacements, but that small systematic dif-

ferences in the overall mean resulting from the process will produce a significant effect on displacements.

That the derived displacements can be very sensitive to small differences in baselines is obvious when considering that the final displacement produced by a shift of δa is $0.5\delta aT^2$—a shift of only $0.1Q = 0.006$ cm/sec^2 (one tenth of a digital count) leads to a final displacement of 59 cm. We show this in Figure 10, which shows displacements obtained from 2001CDxmean acceleration data corrected using the mean computed from the pre-event portion of the data (the first arrival of the event is at 16.655 sec) and using means that differ from that mean by 0.1, 0.2, and 0.3 digital counts. The differences in displacement trends are significant, which again emphasizes the difficulty in obtaining residual displacements from digital data, at least from instruments with no more precision than 16 bits.

A proper model of the differences in the 2001CD and 2001CDxmean data is probably more complicated than the sum of random errors plus a residual bias, and would require modeling the distortions caused by the analog-to-digital conversion (ADC) when applied to slowly varying signals. The differences are probably related to the ADC applied to a signal with a mean level that may be between two digital counts, with added random noise. It is not our intention to explain exactly why the results of the two datasets are different, and the conclusions of our paper stand regardless of which dataset is used. The results in the rest of the paper were prepared using the 2001CD data from Lee *et al.* (2001a); similar results are obtained if the 2001CDxmean data are used.

Figure 11 shows the 5%-damped pseudoacceleration response spectra of the three closely spaced records HWA013, HWA014, and HWA019. Because the response spectra of the two colocated records (HWA019 and HWA2) are similar for periods to 100 sec (Fig. 7), the spectra of HWA2 are not shown in Figure 11. The spectra of different instruments overlap between about 3 sec and 100 sec, as we would expect given the similarity in the sites, the small distances between stations, and the large source-to-site distances. The differences at shorter periods might be due to differences in local-site response, and the differences for periods greater than about 100 sec reflect the dissimilar drifts in the displacements at long times.

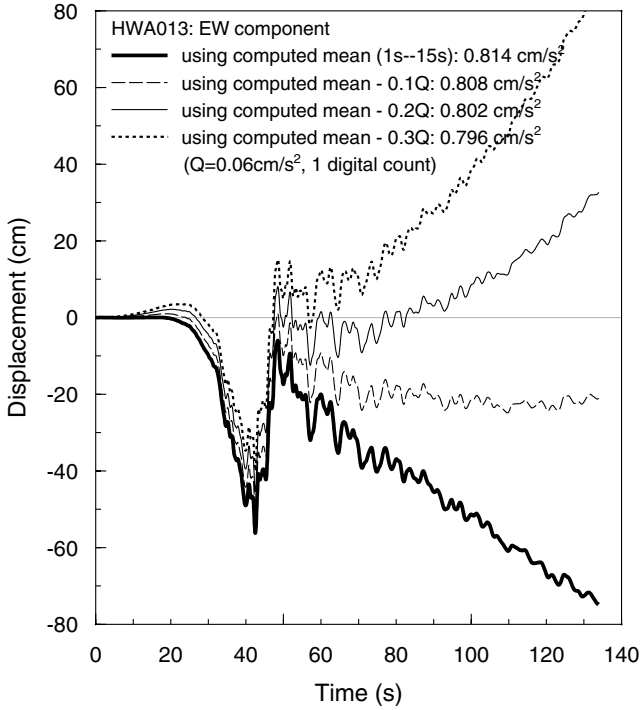

Figure 10. Displacements derived from the HWA013-EW accelerations for a series of means removed from the whole time series. The means include the mean computed from the pre-event portion of the acceleration (from 1 to 15 sec), as well as that mean reduced by fractions of 0.1, 0.2, and 0.3 of one digital count (as given by the quanta Q, which is 0.06 cm/sec^2 per count). The data used were provided by W. Lee (not the data from Lee *et al.*, 2001a).

Correcting for Baseline Offsets

The different characters of the drifts in displacements at long times, even for the same component of motion, implies that the sources of the baseline offsets are a form of instrument "noise"; therefore, it will be difficult, if not impossible, to correct for the offsets so as to obtain the permanent displacements. Despite this, we note that the EW displacement for HWA019 has an apparently linear trend for both the 2001CD and the 2001CDxmean data (Fig. 8e,f), and we explore here whether corrections can be made to recover the real displacements of the east–west component. We conclude that the uncertainties in some of the essential correction parameters make it impossible to recover the displacements in the absence of other information. We follow that work with a discussion of filtering the records to remove the long-period components of motion. The displacements from all of the A-900/A instruments are very similar if energy at frequencies less than about 0.015 Hz is removed.

Linear trends can be produced by a short-duration pulse in accelerogram, whereas parabolic trends are produced by a step in the accelerogram time series. With this interpretation, we have corrected the record of HWA019-EW by assuming that a 1.0-sec pulse occurred in acceleration, with amplitude such that the area of the pulse equals the slope of the line fit to the displacement. Other pulse durations, such as 0.5-, 1.5-, and 2.0-sec durations, give very similar results as long as the areas of the pulses are constant. A longer duration of the pulse corresponds to smaller amplitude. Figure 12a illustrates the displacements integrated from corrected accelerations removing a 1-sec pulse at 20, 55, 65, and 80 sec, respectively. The time at which the pulse occurs is a free parameter. As can be seen, the permanent displacement is highly sensitive to the location of the pulse. Placing the pulse at 65 sec gives good agreement with the coseismic

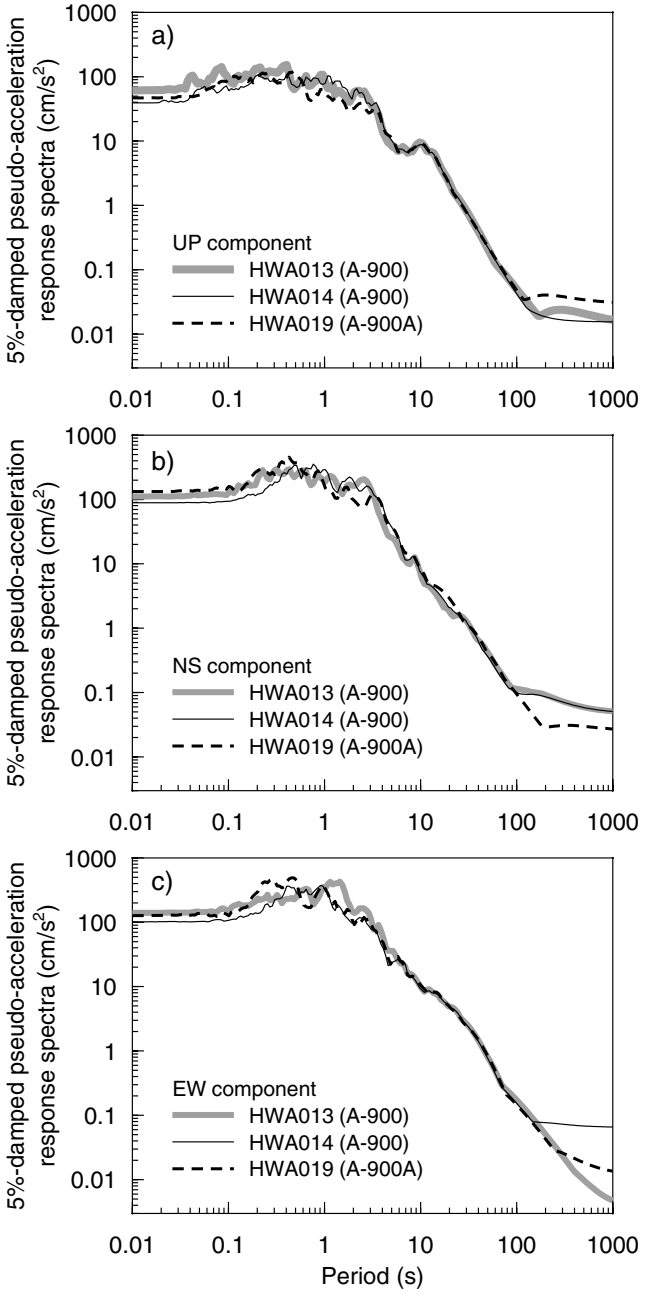

Figure 11. Five percent-damped acceleration response spectra calculated from the uncorrected accelerations recorded by the three closely spaced (but not colocated) instruments HWA013(A-900), HWA014(A-900), and HWA019(A-900A). The response spectra of HWA2 are almost equal to those of HWA019 for periods less than 100 sec and are not shown here. (See Fig. 7 for a comparison over the whole period range.) Before computing the response spectra, zeros were added to the end of the acceleration time series so that the total duration exceeded the oscillator period.

displacement. In many cases, however, closely spaced or colocated stations and GPS station are not available; therefore, there would be no control of the time at which the pulse occurs. Because the higher-frequency shaking had not ceased, we were concerned that the fitted line would be sensitive to the segment of the displacement used in the least-squares fit. We tested this by varying the start time of the fit (*begin_fit*) at 75, 80, 90, 100, and 110 sec, respectively; the slopes of the fitted lines are not sensitive to the line segment used in the fit, and as a result, neither are the corrected displacements (Fig. 12b), mostly because the trend in the displacement-time series is linear and the slope is significant.

Another method for correcting of baseline offsets is a generalization by Boore (1999, 2001) of one proposed by Iwan *et al.* (1985), which assumes that shifts in the baseline occur during some interval of strong shaking and can be accounted for by a pulse followed by a step in acceleration (see Boore, 2001, figure 4 for an example). The duration and location of the pulse is specified by the first and last occurrences of acceleration exceeding a threshold acceleration. Iwan *et al.* (1985) "option 1" used a threshold of 50 cm/sec^2, based on the particular instrument that they studied. Because there is no reason to assume that this threshold applies to the A-900 instruments, we used eight different thresholds: 20, 30, 40, 50, 60, 70, 80, and 90 cm/sec^2, respectively. The results are shown in Figure 13, which shows that the correction is not very sensitive to the choice of the exceedence threshold (Fig. 13d). The corrections, however, are sensitive to the time interval used in determining the straight-line fit, as seen by comparing graphs d and e of Figure 13, which used 90-sec and 100-sec start times, respectively, for fitting the velocity time series. The sensitivity to the start time is due to several factors: 1) the method is based on fitting a straight line to velocity rather than to displacement, as in the previous correction method (Fig. 12b), and the slope of the velocity is very small for the east–west component of HWA019 (the least-squares fitted lines are shown in Fig. 13b,c), and 2) the higher frequency shaking has not ceased, making the slope of the line fitted to velocity sensitive to the continued shaking superimposed on the overall trend.

Both correction schemes (removing a pulse or removing a pulse followed by a step) can produce reasonable displacements that look similar, with a relatively constant displacement after the interval of strong shaking. There is no inconsistency in this result. If the slope of the velocity later in the record is very small, the difference between a parabola and a straight line in the displacement trace is not as pronounced as it would be if the velocity slope were larger. For the same reason, the correction scheme assuming a linear trend, rather than a step in velocity (the method of Iwan *et al.*, [1985], Fig. 13b,c), requires a pulse followed by a very small step in acceleration, just as does the first correction (Fig. 12) method discussed previously. This is shown in Figure 14, which shows the baseline offsets of HWA019-EW corresponding to the two correction schemes considered here—removing a pulse (Fig. 14a) or removing a pulse followed by a step (Fig. 14b). Note the difference in scale for the ordinate of Figure 14a,b (a factor of 5). In addition, note the small amplitudes of the pulses. The pulse heights could be

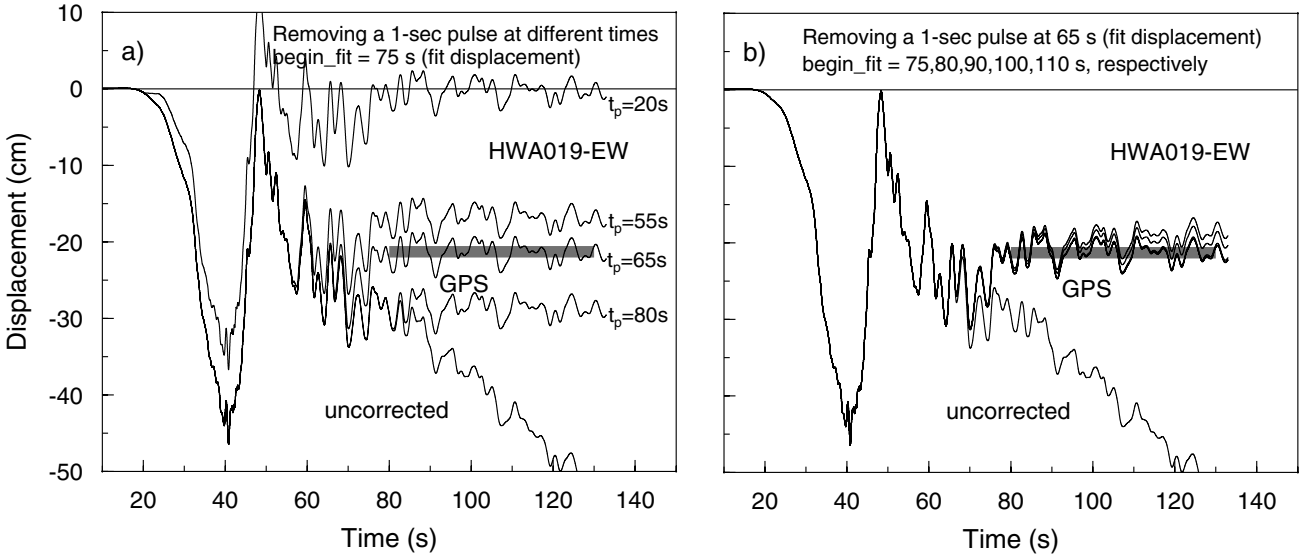

Figure 12. Displacements for HWA019-EW, corrected by assuming a 1-sec pulse in the acceleration baseline. (The area under the pulse produces a step in velocity that corresponds to the slope of a line fit to displacement.) (a) Removing a 1-sec pulse at 20, 55, 65, and 80 sec, respectively. The area of the pulse is constant and equals the slope of the line fitting the displacements from 75 sec to end. (b) Removing a pulse at 65 sec, where the size of the pulse depends on the beginning time used in the least-squares fitting. (The line was fit to the displacements from the beginning time, *begin_fit*, to the end of the record.)

reduced to a fraction of the indicated heights by increasing the pulse duration to maintain the same area under the pulses. These pulses would be difficult to detect by looking at the recorded acceleration time series—the pulses will not stand out as "spikes." Displacements produced by the two baseline correction schemes are shown in Figure 14c,d. The two pulse-followed-by-a-step corrections produce very similar displacements, which are roughly comparable with the displacement produced by the 1-sec pulse located at 65 sec. As shown earlier (Figs. 12a and 13d), the single pulse at 65 sec and the two Iwan step–pulse corrections give reasonable displacements, which agree well with the coseismic displacement.

As we have shown, the problems of baseline offsets generally manifest themselves at long periods. Hence, low-cut filtering is often used to minimize the effects of baseline offsets (e.g., Trifunac, 1971; Converse, 1992; Chiu, 1997; Boore *et al.*, 2002). Such a procedure, however, clearly precludes extracting permanent displacement from the records. In this study, a series of low-cut filters were used to eliminate the baseline offsets occurring in the records of the four A-900/A instruments. Figure 15 shows the filtered displacement waveforms from the four instruments. A fourth-order, butterworth, causal, low-cut filter was used in this study. The agreement between the ground displacements at the three stations has been considerably improved after the low-cut filtering. As the corner frequencies of the filters are increased, the overall waveforms of the different components become more and more consistent. For the two colocated records, a 0.005-Hz low-cut filter can eliminate most of the differences in the overall character of displacement waveforms; a 0.01-Hz low-cut filter produces close agreement for all but the north–south component from HWA013; and a 0.015-Hz low-cut filter brings all of the traces into good overall agreement. Of course, low-cut filtering does not change the relative differences at high frequencies, which are particularly pronounced for the north–south component. The east–west component and, in particular, the up–down component waveforms are in excellent agreement for all frequencies. An example of response spectra for the various low-cut filters is shown in Figure 16. Clearly, the response spectra for periods of engineering concern (e.g., $<$20 sec) are not affected at all by the presence of the long-period noise.

By low-cut filtering with a filter corner of 0.015 Hz or higher, baseline "errors" were eliminated, but of course the energy content below 0.015 Hz was also cut off. We cannot say, however, that the A-900/A instrument is incapable of making useful recordings of motions at frequencies less than about 0.015 Hz; what is important is the relative amplitude of the signal and the "noise". Consider a baseline offset given by a step in acceleration—its Fourier spectrum goes as $1/f$, and therefore, in displacement the spectrum goes as $1/f^3$. So although the effect of the "noise" introduced by the baseline offset exists at all frequencies, it is most important at low frequencies. Whether the "noise" is important for any particular filter cutoff will depend on the amplitude of the signal compared with the noise. A record close to the fault will have a much larger long-period signal than one far away. Therefore, we expect that the frequency at which the

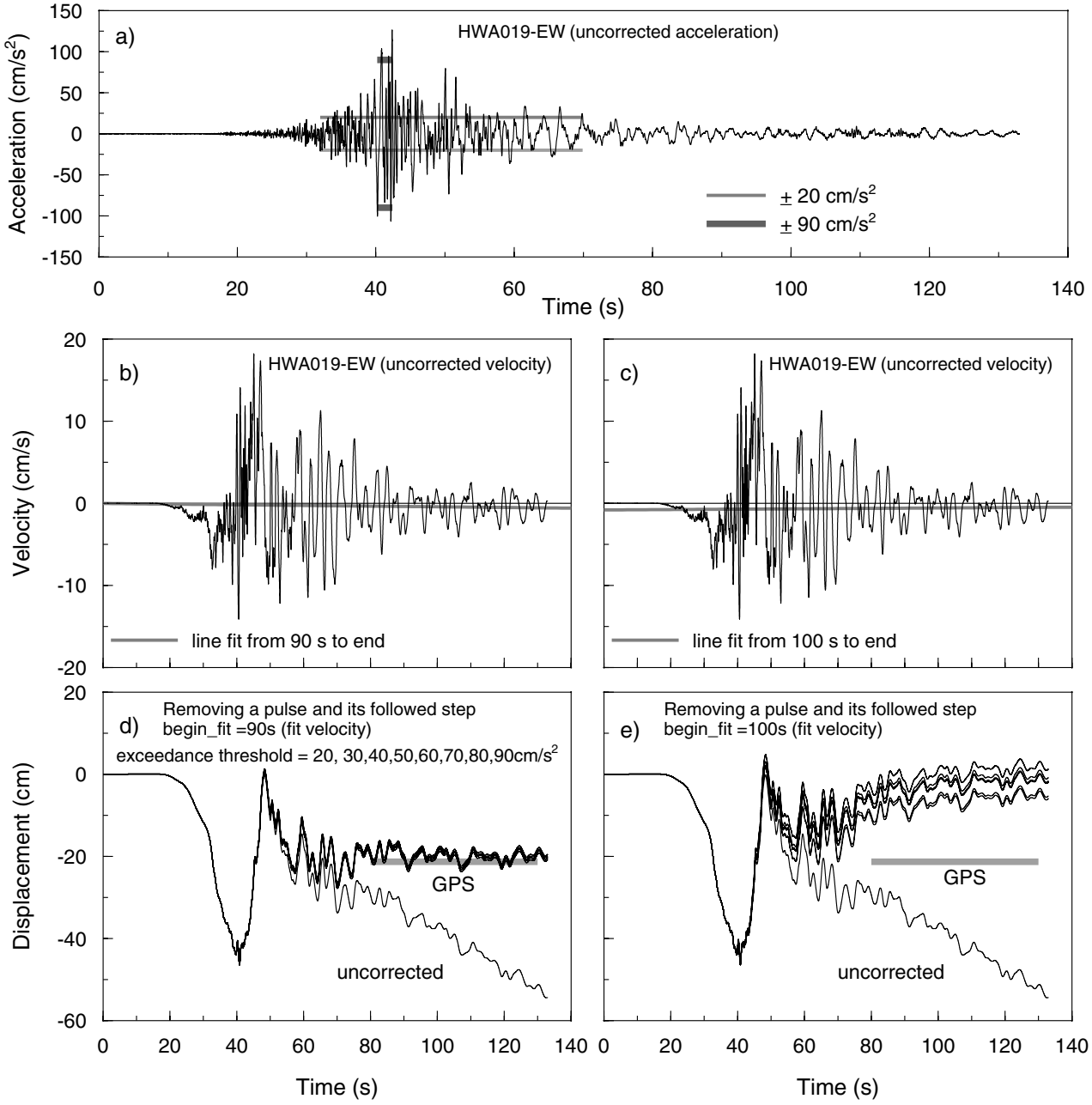

Figure 13. Acceleration, velocity, and displacement time series for the HWA019-EW record, applying an Iwan *et al.* (1985) correction in which a baseline corresponding to a pulse followed by a step in acceleration is removed from the acceleration time series. Exceedance levels of 20, 30, 40, 50, 60, 70, 80, and 90 cm/sec^2 were used. Graph a shows the 20 and 90 cm/sec^2 levels. The velocities are shown in graphs b and c, along with the least-squares lines fit to the later portions of the velocity time series (as indicated on the graphs). The displacements are shown in graphs d and e.

noise overwhelms the signal will be smaller for stations close to the fault than at distant stations.

Discussion and Conclusions

Modern digital instruments have the potential to recover the complete ground displacements from accelerometer records recorded close to large earthquakes, but baseline offsets make it difficult, if not impossible, in many cases to do so. It has been recognized from the time that records from the Chi-Chi mainshock were first available that baseline offsets are common in most records of this event, including those recorded on 24-bit systems (e.g., Boore, 1999, 2001; Wang, 2001; Wang *et al.*, 2001). We also checked some records from aftershocks of this event released by the CWB (Lee *et al.*, 2001b,c). Baseline errors are also present for these after-

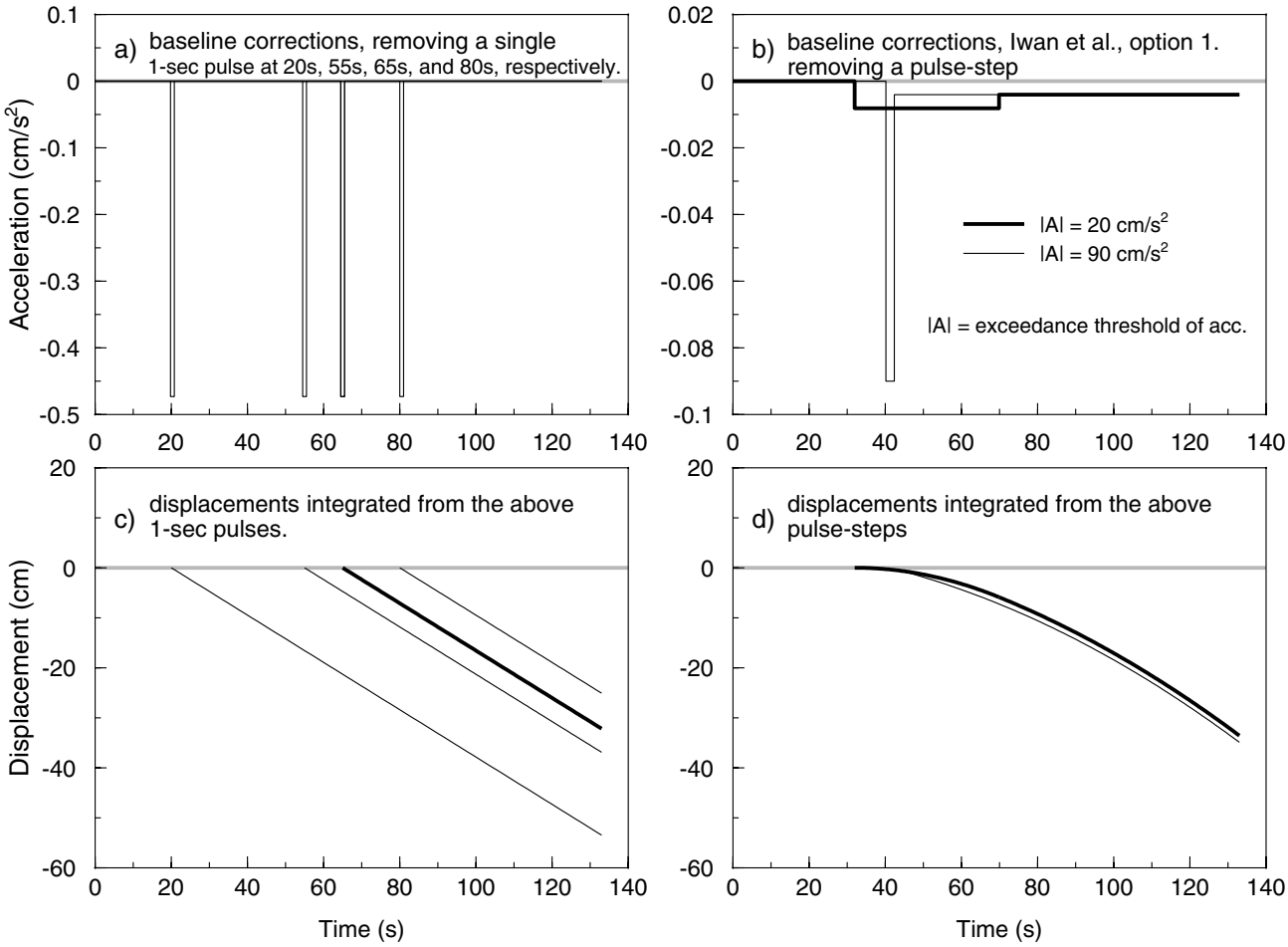

Figure 14. The baseline corrections used to produce the displacements shown in Figures 12 and 13. (a) The single pulses removed from the original baseline of acceleration at 20, 55, 65, and 80 sec, respectively (Fig. 12a); (b) the pulse steps removed from the original baseline of acceleration (Fig. 13d); (c) displacements produced by the pulses illustrated in graph a; (d) displacements produced by the pulse steps illustrated in graph b.

shock records. Furthermore, baseline correction on aftershock records would be more difficult than that for the mainshock records because the pre-event portion of the aftershock records contains motions from previous events in a lot of cases. Although we can say with certainty that baseline offsets are very common in the digital records, it is not clear whether the baseline offsets are due to something within the instruments or are the response to actual ground motion, either elastic, such as rotations, or inelastic, such as slumping or differential compaction, or are result from a combination of sources internal and external to instrument. The observations in this study and our previous studies illustrate the difficulties in understanding the true sources of the baseline offsets occurring in many digital recordings.

For the records used in this study, we find that the baseline offsets differ for each component of an individual accelerograph. Hence, the offsets were most probably produced by some intrinsic mechanism within the instrument, although we do not know the exact mechanism. Because of the random nature of the baseline offsets, we cannot think of a universal correction scheme that can be applied to eliminate the baseline offsets. We recommend low-cut filtering to reduce the effects of baseline offsets but with the resulting loss of information about the permanent displacements. Because it seems that most often the source of the baseline offsets is within the instruments, we hope that the manufacturers will try to fix the problem so that analysis of future recordings can take full advantage of the resolution and bandwidth of the instruments. Another possibility is to follow the suggestion of Clinton and Heaton (2002) and use velocity sensors rather than acceleration sensors to extract information at long periods.

Acknowledgments

We thank W. H. K. Lee for encouraging us in this study, for providing data without the means being removed, and for supplying basic information about the Hualien seismic station. We also thank Shui-Beih Yu for supply-

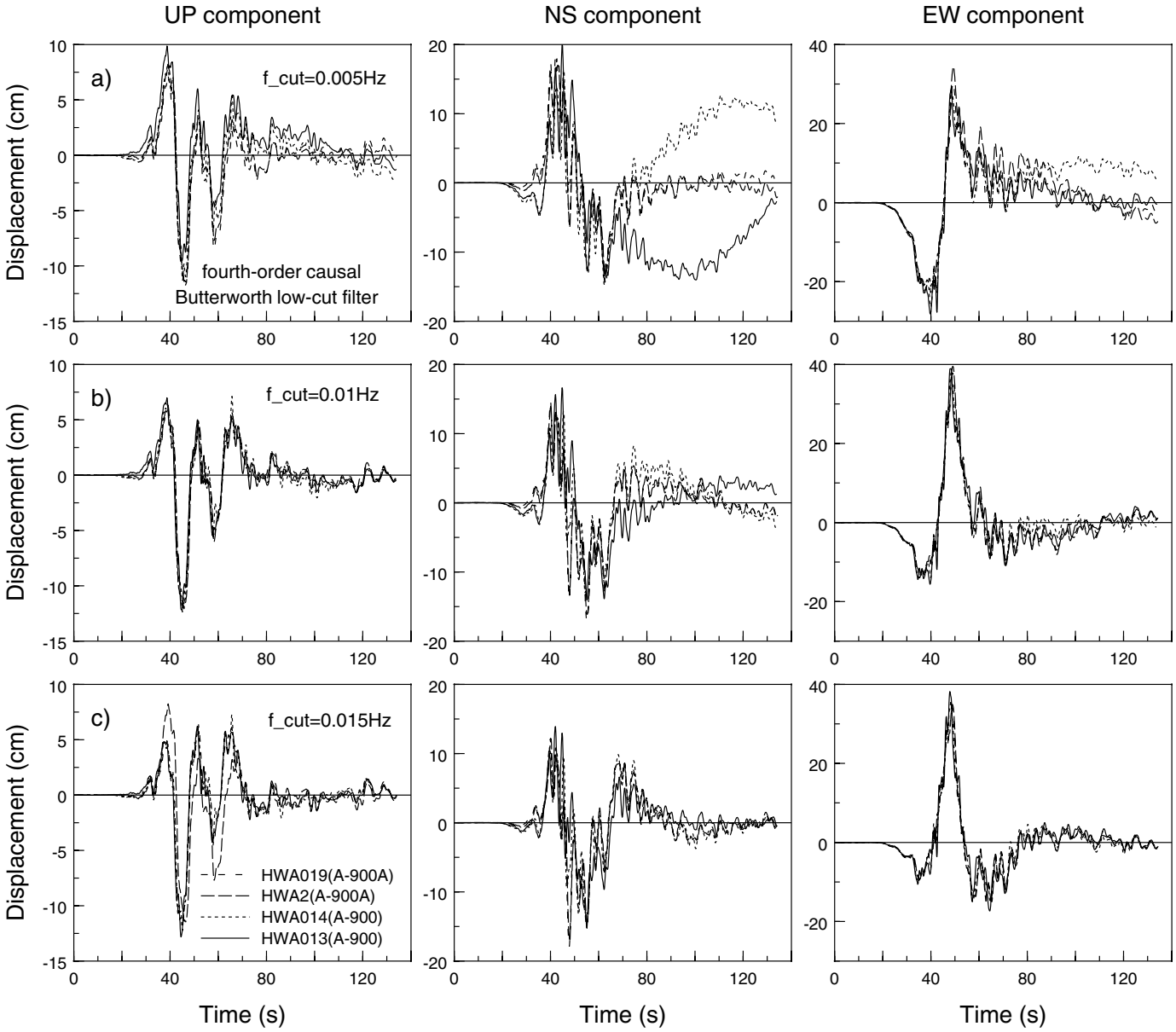

Figure 15. The filtered three-component displacements obtained by integration of the accelerations recorded by the closely spaced instruments HWA013, HWA014, HWA019, and HWA2 (the latter two are colocated). A fourth-order butterworth causal low-cut filter was applied to the uncorrected accelerations. (a) 0.005-Hz low-cut filter; (b) 0.01-Hz low-cut filter; (c) 0.015-Hz low-cut filter.

ing the coseismic displacement information. Discussions with John Evans, Chris Stephens, and Francis Wu were useful. The careful corrections and thoughtful suggestions of Chris Stephens, Chuck Mueller, and M. I. Todorovska are deeply appreciated, as was the constructive review of one anonymous reviewer. The Central Weather Bureau of Taiwan and W. H. K. Lee and colleagues deserve praise for funding, installing, and maintaining the strong-motion network and for making the data from the mainshock freely available soon after the earthquake. This research was partially funded by the Natural Science Foundation of China under Project No. 50178007. The first author wishes to acknowledge the German Academic Exchange Service (DAAD) for funding through the International Quality Network: Georisks (http://www.iqn-georisk.de).

References

Abrahamson, N. A., and D. Sykora (1993). Variations of ground motions across individual sites, in *Proc. of the DOE Natural Phenomena Hazards Mitigation Conf.*, Atlanta, Georgia, 1 October 1993, 192–198.

Amini, A., and M. D. Trifunac (1985). Analysis of a force balance accelerometer, *Soil Dyn. Earthquake Eng.* **4,** 82–90.

Boore, D. M. (1999). Effect of baseline corrections on response spectra for two recordings of the 1999 Chi-Chi, Taiwan, earthquake, *U.S. Geol. Surv. Open-File Rept. 99-545.*

Boore, D. M. (2001). Effect of baseline correction on displacement and response spectra for several recordings of the 1999 Chi-Chi, Taiwan, earthquake, *Bull. Seism. Soc. Am.* **91,** 1199–1211.

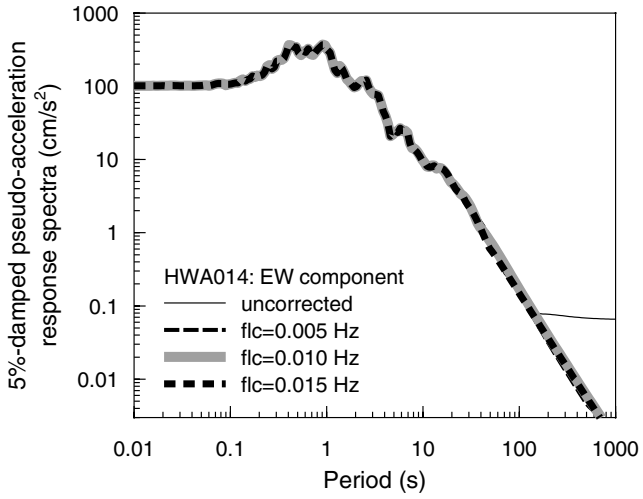

Figure 16. Five percent-damped pseudoacceleration response spectra calculated from the uncorrected acceleration time series and a series of low-cut filtered acceleration time series (fourth-order butterworth causal low-cut filter, fcut = 0.005, 0.010, and 0.015 Hz) recorded by the EW component of HWA014 (A-900).

Boore, D. M. (2003). Analog-to-digital conversion as a source of drifts in displacements derived from digital recordings of ground acceleration, *Bull. Seism. Soc. Am.* **93,** (submitted for publication).

Boore, D. M., C. D. Stephens, and W. B. Joyner (2002). Comments on baseline correction of digital strong-motion data: examples from the 1999 Hector Mine, California, earthquake, *Bull. Seism. Soc. Am.* **92,** 1543–1560.

Bradner, H., and M. Reichle (1973). Some methods for determining acceleration and tilt by use of pendulums and accelerometers, *Bull. Seism. Soc. Am.* **63,** 1–7.

Building Seismic Safety Council (1998). 1997 Edition NEHPR Recommended Provisions for Seismic Regulations for New Buildings, FEMA 302/303, developed for the Federal Emergency Management Agency, Washington, D.C.

Chiu, H. C. (1997). Stable baseline correction of digital strong-motion data, *Bull. Seism. Soc. Am.* **87,** 932–944.

Chiu, H. C. (2001). Recovery of coseismic ground motions with permanent displacement from the strong-motion data of the 1999 Chi-Chi, Taiwan Earthquake (abstract), *Seism. Res. Lett.* **72,** 235–236.

Clinton, J. F., and T. H. Heaton (2002). Potential advantages of a strong-motion velocity meter over a strong-motion accelerometer, *Seism. Res. Lett.* **73,** 332–342.

Converse, A. M. (1992). BAP–Basic strong-motion accelerogram processing software; Version 1.0, *U.S. Geol. Surv. Open-File Rept. 92-296A*.

Evans, J. R. (2001). Wireless monitoring and low-cost accelerometers for structures and urban sites, in *Strong Motion Instrumentation for Civil Engineering Structures, Proc., NATO Advanced Research Workshop*, Istanbul, 2–5 June 1999, M. Erdik, M. Celebi, and V. Mihailov (Editors), Kluwer Academic Publishers, Netherlands, 229–242.

Field, E. H., and S. E. Hough (1997). The variability of PSV response spectra across a dense array deployed during the Northridge aftershock sequence, *Earthquake Spectra* **13,** 243–258.

Graizer, V. M. (1979). Determination of the true ground displacement by using strong motion records, *Bull. Acad. Sci. USSR Phys. Solid Earth* **15,** 875–885.

Hanks, T. C. (1975). Strong ground motion of the San Fernando, California, earthquake: ground displacements, *Bull. Seism. Soc. Am.* **65,** 193–235.

Iwan, W. D., M. A. Moser, and C.-Y. Peng (1985). Some observations on strong-motion earthquake measurement using a digital accelerograph, *Bull. Seism. Soc. Am.* **75,** 1225–1246.

Lee, W. H. K., T. C. Shin, K. W. Kuo, and K. C. Chen (1999). *CWB Free-Field Strong-Motion Data from the 921 Chi-Chi Earthquake*, Vol. 1. Digital acceleration files on CD-ROM, prepublication version, Seismology Center, Central Weather Bureau, Taipei, Taiwan, 6 December 1999.

Lee, W. H. K., T. C. Shin, K. W. Kuo, K. C. Chen, and C. F. Wu (2001a). *CWB Free-Field Strong-Motion Data from the 921 Chi-Chi Earthquake: Processed Acceleration Files on CD-ROM*, CWB Strong-Motion Data Series CD-001, Seismological Observation Center, Central Weather Bureau, Taipei, Taiwan, 31 March 2001.

Lee, W. H. K., T. C. Shin, and C. F. Wu (2001b). *CWB Free-Field Strong-Motion Data from Three Major Aftershocks of the 1999 Chi-Chi Earthquake: Processed Acceleration Data Files on CD-ROM*, CWB Strong-Motion Data Series CD-002, Seismological Observation Center, Central Weather Bureau, Taipei, Taiwan, 28 August 2001.

Lee, W. H. K., T. C. Shin, and C. F. Wu (2001c). *CWB Free-Field Strong-Motion Data from 30 Early Aftershocks of the 1999 Chi-Chi Earthquake: Processed Acceleration Data Files on CD-ROM*, CWB Strong-Motion Data Series CD-003, Seismological Observation Center, Central Weather Bureau, Taipei, Taiwan, 31 August 2001.

Lee, C. T., C. T. Cheng, C. W. Liao, and Y. B. Tsai (2001d). Site classification of Taiwan free-field strong-motion stations, *Bull. Seism. Soc. Am.* **91,** 1283–1297.

Liu K.-S., T.-C. Shin, and Y.-B. Tsai (1999). A free-field strong motion network in Taiwan, *TSMIP, Terr., Atmospher. Oceanic Sci.* **10,** 377–396.

Novikova E. I., and M. D. Trifunac. (1992). Digital instrument response correction for the force-balance accelerometer, *Earthquake Spectra* **8,** 429–442.

Shakal, A. F., and C. D. Petersen (2001). Acceleration offsets in some FBA's during earthquake shaking (abstract), *Seism. Res. Lett.* **72,** 233.

Shin T.-C, K. W. Kuo, W. H. K. Lee, T.-L. Teng, and Y. B. Tsai (2000). A preliminary report on the 1999 Chi-Chi (Taiwan) earthquake, *Seism. Res. Lett.* **71,** 24–30.

Shin, T. C., F. T. Wu, J. K. Chung, R. Y. Chen, Y. M. Wu, C. S. Chang, and T. L. Teng (2001). Ground displacements around the fault of the September 20th, 1999, Chi-Chi Taiwan earthquake, *Geophys. Res. Lett.* **28,** 1651–1654.

Todorovska, M. I., E. I. Novikova, M. D. Trifunac, and S. S. Ivanovic (1995). Correction for misalignment and cross axis sensitivity of strong earthquake motion recorded by SMA-1 accelerographs, University of Southern California, Report No. CE 95-06, Los Angeles, California.

Todorovska, M. I. (1998). Cross-axis sensitivity of accelerographs with pendulum like transducers–mathematical model and the inverse problem, *Earthquake Eng. Struct. Dyn.* **27,** 1031–1051.

Trifunac, M. D. (1971). Zero baseline correction of strong-motion accelerograms, *Bull. Seism. Soc. Am.* **61,** 1201–1211.

Trifunac, M. D., and M. I. Todorovska (2001). A note on the useable dynamic range of accelerographs recording translation, *Soil Dyn. Earthquake Eng.* **21**, 275–286.

Wang, G.-Q. (2001). The characteristics of near-fault ground motion caused by the 1999, Chi-Chi, Taiwan earthquake, *Ph.D. thesis*, Institute of Geology, China Seismological Bureau (in Chinese).

Wang, G.-Q, X. Y. Zhou, Z. J. Ma, and P. Z. Zhang (2001). Data files from "A preliminary study on the randomness of response spectra of the 1999 Chi-Chi, Taiwan, Earthquake", *Bull. Seism. Soc. Am.* **91,** 1388–1389.

Wang, G.-Q, X. Y. Zhou, P. Z. Zhang, and H. Igel (2002). Characteristics of amplitude and duration for near fault strong ground motion from the 1999 Chi-Chi, Taiwan, Earthquake, *Soil Dyn. Earthquake Eng.* **22,** 73–96.

Wong, H. L., and Trifunac, M. D. (1977). Effects of cross-axis sensitivity and misalignment on response of mechanical-optical accelerographs, *Bull. Seism. Soc. Am.* **67,** 929–956.

Yu, S.-B., L.-C. Kuo, Y.-J. Hsu, H.-H. Su, and C.-C. Liu (2001). Preseismic deformation and coseismic displacements associated with the 1999 Chi-Chi, Taiwan Earthquake, *Bull. Seism. Soc. Am.* **91,** 995–1012.

Institute of Geophysics
University of Munich
Munich, 80333 Germany
wang@geophysik.uni-muenchen.de
igel@geophysik.uni-muenchen.de
(G.-Q.W., H.I.)

U.S. Geological Survey, MS 977
345 Middlefield Road
Menlo Park, California 94025
boore@usgs.gov
(D.M.B.)

College of Architectural and Civil Engineering
Beijing Polytechnic University
Beijing, 100022 People's Republic of China
zhouxy@solaris.bjpu.edu.cn
(X.-Y.Z., G.-Q.W.)

Manuscript received 24 January 2002.

Appendix

Table A1

Peak Ground Accelerations Recorded by the 22 A-800–A-900A Pairs in the Chi-Chi Earthquake

Station	Site Class*	Lat. (°N)	Long. (°E)	Elev. (km)	Epdist.† (km)	Drup.‡ (km)	PGA UP (cm/sec²)	PGA NS (cm/sec²)	PGA EW (cm/sec²)	Instrument Model
WNT	D	23.8783	120.6843	0.11	11.9	2.21	−310.60	−602.00	−920.70	A-800
TCU129	D	23.8783	120.6843	0.11	11.9	2.21	−335.00	−610.60	−982.90	A-900A
TCU	D	24.1475	120.676	0.084	34.2	4.47	−118.20	−186.60	−201.00	A-800
TCU082	D	24.1475	120.676	0.084	34.2	4.47	−129.30	192.40	−221.00	A-900A
NSY	C	24.4162	120.7607	0.311	61.7	9.08	−84.20	−150.30	118.70	A-800
TCU128	C	24.4162	120.7607	0.311	61.7	9.08	−90.38	−162.90	141.10	A-900A
WGK	D	23.6862	120.5622	0.075	30.9	13.31	175.60	446.00	337.80	A-800
CHY101	D	23.6862	120.5622	0.075	30.9	13.31	162.10	390.10	−332.70	A-900A
ALS	C	23.5103	120.8052	2.413	38.8	14.37	85.65	−145.50	212.90	A-800
CHY074	C	23.5103	120.8052	2.413	38.8	14.37	101.30	158.50	234.60	A-900A
WTP	B	23.2455	120.6138	0.56	70.7	41.89	30.00	43.55	44.50	A-800
CHY102	B	23.2455	120.6138	0.56	70.7	41.89	−23.15	48.45	40.49	A-900A
ESL	D	23.8137	121.4328	0.178	64.7	44.71	56.45	72.25	−66.55	A-800
HWA020	D	23.8137	121.4328	0.178	64.7	44.71	52.46	66.63	−56.58	A-900A
WSF	E	23.638	120.2217	0.006	63.8	47.71	32.06	66.99	−64.60	A-800
CHY076	E	23.638	120.2217	0.006	63.8	47.71	31.40	−70.94	−68.61	A-900A
NSK	B	24.6755	121.3583	0.682	106.6	48.02	39.72	−53.59	−67.95	A-800
TCU085	B	24.6755	121.3583	0.682	106.6	48.02	41.39	−52.34	−62.09	A-900A
STY	B	23.1625	120.7573	0.64	77.4	50.29	−19.62	39.24	−36.37	A-800
KAU050	B	23.1625	120.7573	0.64	77.4	50.29	22.97	37.14	−41.69	A-900A
HSN	D	24.8022	120.9695	0.034	105.7	53.16	−26.32	−79.91	54.07	A-800
TCU081	D	24.8022	120.9695	0.034	105.7	53.16	−36.13	93.13	76.68	A-900A
HWA	D	23.977	121.605	0.016	83	54.47	42.59	−107.62	119.14	A-800
HWA019	D	23.977	121.605	0.016	83	54.47	46.79	−133.57	126.46	A-900A
HWA2	D	23.977	121.605	0.016	83	54.47	47.73	−132.19	129.08	A-900A
SGS	B	23.0817	120.5827	0.278	89	60.29	−19.14	−37.80	−28.23	A-800
KAU047	B	23.0817	120.5827	0.278	89	60.29	20.28	−41.93	−32.60	A-900A
ENA	B	24.428	121.7407	0.113	114.5	66.3	53.59	64.60	63.64	A-800
ILA050	B	24.428	121.7407	0.113	114.5	66.3	53.35	62.81	−63.58	A-900A
CHK	D	23.0992	121.3653	0.034	102.2	68.29	−11.96	45.46	−65.56	A-800
TTN014	D	23.0992	121.3653	0.034	102.2	68.29	−25.18	43.60	−49.11	A-900A
NCU	D	24.97	121.1867	0.134	129	73.03	−34.45	98.57	−79.43	A-800
TCU083	D	24.97	121.1867	0.134	129	73.03	−33.08	114.70	−89.24	A-900A
TAI1	D	23.0402	120.2283	0.008	108	79.31	−20.10	−44.02	87.57	A-800
CHY078	D	23.0402	120.2283	0.008	108	79.31	−20.94	−43.78	86.85	A-900A
TTN	D	22.754	121.1465	0.009	127.6	96.67	14.36	−29.19	29.19	A-800
TTN015	D	22.754	121.1465	0.009	127.6	96.67	−14.12	−30.63	25.36	A-900A
SGL	D	22.7252	120.4908	0.03	129.6	100.83	8.61	−30.15	−28.23	A-800
KAU048	D	22.7252	120.4908	0.03	129.6	100.83	−11.78	28.65	38.28	A-900A
PNG	B	23.5672	119.5552	0.011	131	115.8	−14.36	32.54	−29.19	A-800
CHY075	B	23.5672	119.5552	0.011	131	115.8	15.19	37.03	−37.03	A-900A
TAW	B	22.3575	120.8957	0.008	166.7	138.98	−3.35	−5.26	5.26	A-800
TTN016	B	22.3575	120.8957	0.008	166.7	138.98	−6.04	−9.75	−7.24	A-900A
HEN	D	22.0055	120.738	0.022	205.5	178.16	9.09	−24.88	−22.01	A-800
KAU046	D	22.0055	120.738	0.022	205.5	178.16	7.84	−22.49	22.25	A-900A

*National Earthquake Hazards Reduction Program Site Class Scheme (BSSC, 1998).
†Epdist, distance (km) from the Chi-Chi epicenter (23.8603° N, 120.7995° E).
‡Drup, the shortest distance between the station and the fault rupture surface.